ENVIRONMENTAL RESEARCH
CLIMATE

PURPOSE-LED PUBLISHING™ Part of the ENVIRONMENTAL RESEARCH SERIES

PAPER • OPEN ACCESS

The flip side of destructive wildfires: a water supply buffer to climate change

To cite this article: Diana Zamora-Reyes *et al* 2026 *Environ. Res.: Climate* **5** 045015

View the article online for updates and enhancements.

You may also like

- Autler–Townes splitting in Rydberg atoms: transition dipole matrix element extraction and field efficiency analysis
Brian C Holloway, Gavin M Chase, Lee E Harrell et al.
- ICRH modelling of DTT in full power and reduced-field plasma scenarios using full wave codes
A Cardinali, C Castaldo, F Napoli et al.
- Co-design and implementation of community-based flood early warning systems in eastern Argentina
Federico Robledo, Diego Moreira, Camila Prudente et al.

This content was downloaded from IP address 76.149.23.244 on 05/11/2026 at 00:59

ENVIRONMENTAL RESEARCH
CLIMATE

Check for updates

PAPER

OPEN ACCESS

RECEIVED
17 July 2025

REVISED
28 August 2026

ACCEPTED FOR PUBLICATION
18 September 2026

PUBLISHED
16 October 2026

Original content from this work may be used under the terms of the Creative Commons Attribution 4.0 licence.

Any further distribution of this work must maintain attribution to the author(s) and the title of the work, journal citation and DOI.

The flip side of destructive wildfires: a water supply buffer to climate change

Diana Zamora-Reyes[1,*], **Michelle Stern**[1,4], **Lorraine E Flint**[2] **and Whitney Seymour**[3]

[1] US Geological Survey, California Water Science Center, 6000 J St, Sacramento, CA 95819, United States of America
[2] Earth Knowledge Inc., PO Box 3074, Tucson, AZ 85716, United States of America
[3] US Geological Survey, California Water Science Center, 4165 Spruance Rd, San Diego, CA 92101, United States of America
[4] Present address: Delta Stewardship Council, 715 P St, Sacramento, CA 95814, United States of America.
[*] Author to whom any correspondence should be addressed.

E-mail: dzamora-reyes@usgs.gov

Keywords: basin characterization model (BCM), Feather River watershed, wildfire, streamflow, soil moisture, evapotranspiration

Supplementary material for this article is available online

Abstract

Wet to dry climate extremes in California have directly or indirectly impacted droughts, wildfires, and floods, resulting in costly damage. Reservoirs in California were built to store snowpack into the summer and provide multiple benefits in the state: they offer municipal and agricultural water resources during the dry season and prevent flooding downstream. The upper Feather River watershed, which drains 9300 square kilometers (km^2) into Lake Oroville, provides water to over 27 million people and 3000 km^2 of farmland. The North Complex Fire in 2020 and the Dixie and Sugar Fires in 2021 burned over 50% of the watershed, and their long-term impact on the upper Feather River water supply was previously unknown. This study quantified post-wildfire (postfire) changes in plant water use, soil moisture, and streamflow due to changes in vegetation using a physically based water balance model. Long-term trends revealed decreases in annual precipitation and mid- to high-elevation snowpack in this watershed from 1981 to 2020. Due to changes in vegetation, annual postfire streamflow at Feather River at Oroville increased by 22%, 32%, and 16% while summer baseflows increased by 5%, 12%, and 2% in water years (WYs) 2022 through 2024, respectively. Larger increases in streamflow occurred during WY 2023, an extremely wet year relative to the other years, highlighting the challenges in quantifying and managing hydrologic systems with naturally high interannual variability. Seasonal soil moisture increased by up to 34% depending on the location, predominantly in fall and summer postfire. Despite observed historical decreases in precipitation and snowpack, changes in vegetation due to wildfires or other disturbances may increase water availability, and continued management of mixed-conifer forests (i.e. thinning and controlled burns) may help offset future reduced precipitation and snowpack and therefore increase water supply resilience.

1. Introduction

California's extreme weather phenomena—cycles of floods, droughts, and wildfires—have increased in frequency over the past few decades, especially as climate change has increased the likelihood of these events in the present and future (Goss *et al* 2020, Michaelis *et al* 2022, Williams *et al* 2022). The literature suggests that increases in temperature and vapor pressure deficit since 1984 have led to enhanced dryness of vegetation, which in turn has doubled the forest fire area across the western United States compared to natural climate variability alone (Abatzoglou and Williams 2016). The situation is even more pronounced in California, where beneficial autumnal rains that help reduce fire risk have shifted by almost a month since the 1960s and have concentrated most of the annual precipitation in December–March (Luković *et al* 2021). Increasing precipitation variability across the state throughout

Not subject to copyright in the USA. Contribution of U.S. Geological Survey.

the 20th century—driven by wetter extremes, defined as events higher than the 90th percentile—is further complicating these dynamics (Zamora-Reyes *et al* 2022). The confluence of all these variables has resulted in even more complex interactions between the landscape and the availability of the water supply in northern California.

Forested lands in the western United States provide about 65% of the water supply (Brown *et al* 2008), and in California, the upper Feather River watershed is an important region for water and hydropower resources (Koczot *et al* 2005). Located in the northern Sierra Nevada mountains, this snow-dominated watershed delivers resources to about 27 million Californians and more than 3000 square kilometers (km^2) of farmland through the State Water Project (SWP; California Department of Water Resources (DWR) 2025a). Drought-inducing fluctuations in precipitation have outsized impacts downstream on water rights allocations for the $50 billion agricultural industry of the Central Valley and the cities that depend on surface water delivery (Escriva-Bou *et al* 2022, Peterson *et al* 2023). The California DWR operates the SWP and traditionally uses snowpack and snow water equivalent (SWE) measurements as a metric to forecast runoff and anticipate water supply for the dry summer months (California DWR 2025b). However, after consecutive drought years, dry soils across the watershed act as a sponge, substantially absorbing rain and snowmelt and reducing the amount of water that could have reached reservoirs (Lapides *et al* 2022). The upper Feather River watershed has also been affected by large and intense wildfires in the last few years, which can alter hydrological processes within the basin (Walters *et al* 2024).

The North Complex Fire during the summer of 2020 and the Dixie and Sugar Fires in fall 2021 burned a total of 52% of the upper Feather River watershed (figure 1). The North Complex Fire, originally a collection of 21 wildfires that started in the Plumas and Lassen National Forests, was started by lightning from a dry thunderstorm that ignited and burned 1290 km^2 from 17 August to 3 December 2020, with 16 fatalities and 2455 structures destroyed (Safford *et al* 2022). About 47% of the vegetation within this wildfire footprint was classified as having high soil burn severity, while 25% had moderate, 24% had low, and 5% remained unburned (United States Geological Survey (USGS) Nelson K *et al* 2022). The following year, the Sugar Fire started on 2 July 2021 in the Plumas National Forest, while the Dixie Fire ignited a few days later, on 13 July 2021; both fires were extinguished by 25 October 2021 (Taylor *et al* 2022). The soil burn severity distribution within these two wildfires was different from the North Complex Fire; 24% of the area had a high soil burn severity, 29% moderate, 38% low, and 12% was unburned (USGS Nelson K *et al* 2022 flows, and hillslope erosion). The main vegetation type that was burned across all fires was Sierran mixed conifer, consisting of 42% for the North Complex Fire and 51% for the Sugar and Dixie Fire footprints (figure S1, CALFIRE 2015). Other main vegetation types that were burned in the North Complex Fire were White fir (15%), Montane hardwood (12%), and Montane hardwood-conifer (12%; figure S1, CALFIRE 2015). The main vegetation types after Sierran mixed conifer for the Sugar and Dixie Fires were Eastside pine (10%), White fir (9%), and Montane chaparral (6.4%; figure S1; CALFIRE 2015). As of 2024, the Dixie Fire was the second largest (3750 km^2) and the most expensive ($637 million in suppression costs) fire in California's history (Taylor *et al* 2022). Additionally, these fires have negatively impacted water and air quality, affecting various metropolitan areas in northern California such as San Francisco Bay and Sacramento Valley (Carreras-Sospedra *et al* 2024, Dahm *et al* 2025).

These major fire events illustrate the lasting effects of past fire-suppression policies of the 1900s, including the lack of fuel management, combined with present-day conditions that promote extreme fire weather and increased fire season length, such as increasing air temperatures, low humidity caused by decreases in autumn precipitation, and dry vegetation (Taylor and Beaty 2005, Goss *et al* 2020, Safford *et al* 2021, Taylor *et al* 2022, MacDonald *et al* 2023). On a shorter timescale, these major fires were influenced by back-to-back local extreme weather conditions—a wetter than average winter in 2017 and drier than average winters in 2020 and 2021—where fine fuels (e.g. grasses) had the chance to grow after the wet winters, while the understory vegetation had a prolonged amount of time to dry out during the extended hot and dry springs, summers, and autumns (Taylor and Beaty 2005, California DWR 2018, 2021, 2022, Swain 2021). Some studies show no relationship between burn severity and post-wildfire (postfire) runoff (Vieira *et al* 2015, Wu *et al* 2021), but others show that high burn severity leads to increased runoff and decreased evapotranspiration (ET) postfire (Moazeni and Cerdà 2024), slower plant recovery (Mayor *et al* 2007), and decreased infiltration rates (Moody *et al* 2016). Moreover, the impact of wildfire extent and severity on the water balance has been understudied (Moazeni and Cerdà 2024).

Wildfires burn and change the vegetation distribution and surface soil properties of an area depending on fire severity and antecedent moisture conditions. For example, vegetation mortality has the potential to change the water balance as ET is reduced (DeBano *et al* 1998), though the resulting relationship could be more convoluted depending on the ecosystem (Massmann *et al* 2019). A literature review

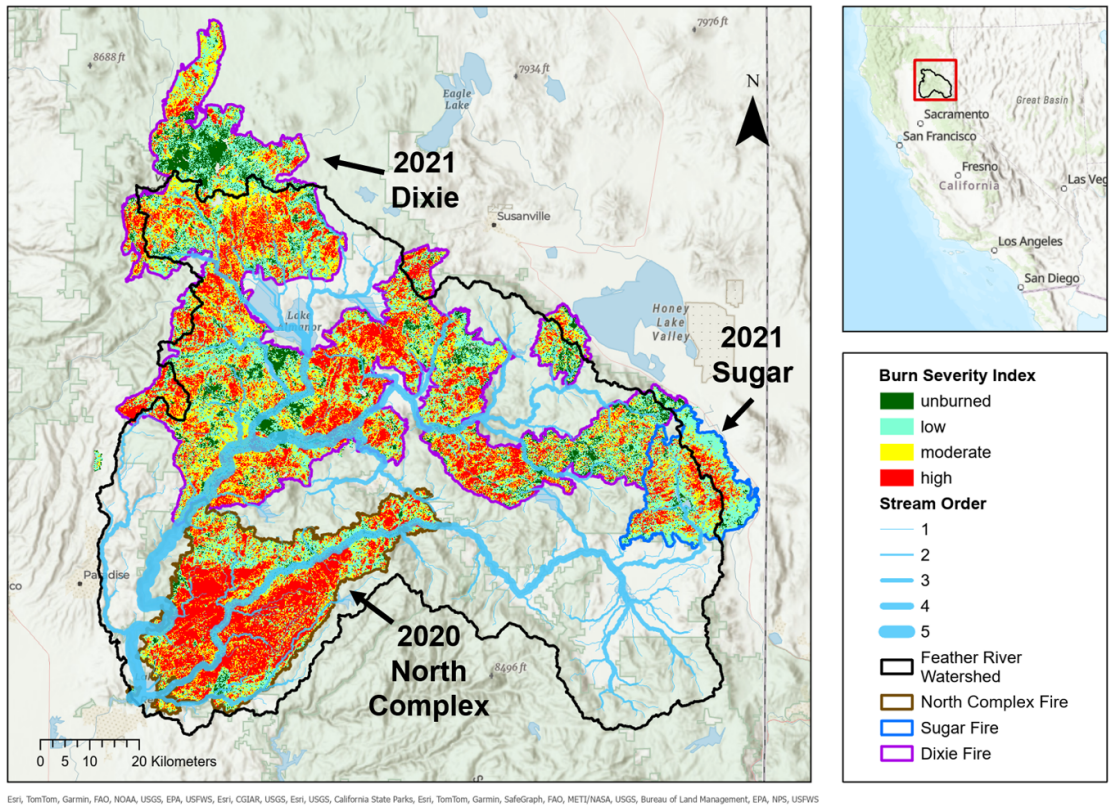


Figure 1. Study area map of the upper Feather River watershed with the burn severity index after the North Complex Fire (brown outline) in 2020 and the Sugar (blue outline) and Dixie (purple outline) Fires in 2021; burn severity index raster data were downloaded from the Monitoring Trends in Burn Severity website (https://mtbs.gov). Also shown is the stream order (aqua lines), which was produced using the USGS 30 m digital elevation model.

focused on western conifer forests in the United States found that this type of stand-replacing disturbance that decreases ET typically led to increases in streamflow but could also lead to decreases or no changes depending on watershed characteristics postfire, such as rapid regrowth and vegetation type (Goeking and Tarboton 2020). In the western United States, several studies found an increase in runoff following wildfires in semi-arid regions (Kinoshita and Hogue 2011, 2015, Williams *et al* 2022) and a snow-dominated region within Yosemite National Park in the central part of the state (Boisramé *et al* 2019). Wildfires can also lead to soil water repellency (hydrophobicity) to depths of several centimeters that can last several years, depending on many factors including the burn severity and soil properties (Debano 2000, Doerr *et al* 2009, Tinebra *et al* 2019, Caltabellota *et al* 2022). However, results from field studies of hydrophobicity tend to vary postfire; hydrophobicity has often been found to be spatially patchy and non-continuous and can also vary temporally and in intensity (DeBano 1998). Other impacts from wildfires on the components of the eco-hydrosphere include loss of surface cover and increases in ash, resulting in soil sealing (Larsen *et al* 2009), decreased water quality (Smith *et al* 2011, Rust *et al* 2018, Magliozzi *et al* 2024), flash floods, debris flows, and hillslope erosion (Ebel *et al* 2012, 2017, Santi and Morandi 2013, Saxe *et al* 2018, Blount *et al* 2020, Ebel 2020, Dow *et al* 2024).

Recent modeling studies in California have mostly focused on estimating ET through remotely sensed data and quantifying changes to the water balance after wildfires (Ma *et al* 2020, Walters *et al* 2024). A previous study evaluated the hydrologic impact of the North Complex and Dixie Fires (as well as the Camp Fire in 2018) on the hydrology of the upper Feather River watershed using only remotely sensed data and found increased soil moisture due to decreases in vegetation and ET following the fires (Walters *et al* 2024). However, the normalized difference vegetation index (NDVI) used for the study may not capture vegetation density or health accurately in evergreen forests as the NDVI tends not to change throughout the year and can be somewhat stable (Ukasha *et al* 2022). Moreover, it has been suggested that modeling studies focused on the relationship between wildfires and their hydrologic impact should emphasize integration of vegetation regrowth, which may have a stronger influence on streamflow dynamics than climate alone (Bart *et al* 2016, Ebel *et al* 2023). Other studies have suggested a focused understanding of the impact of wildfires on water balance dynamics using quantitative analysis, such as the leaf area index (LAI), compared to categorical or qualitative analyses (Goeking and Tarboton 2020).

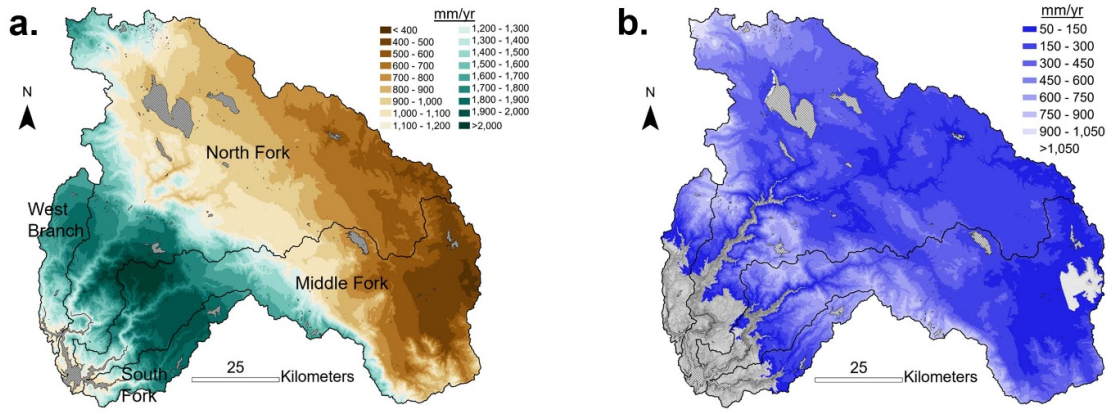


Figure 2. Average annual precipitation (a) and SWE (b) in the upper Feather River watershed for water years 1991–2020. Map (a) was created using monthly data summarized from the Parameter-elevation Regressions on Independent Slopes Model (Daly *et al* 2008), which were downscaled to 30 m grids, while map (b) was created using data calculated by the BCM (Flint *et al* 2021) in millimeters per year (mm/yr).

In evergreen forests, the LAI has a seasonal cycle, where the lowest values are in the winter and the highest values in the summer (Ukasha *et al* 2022).

We applied the Basin Characterization Model (BCM), a physically based water balance model, to quantify changes in ET, soil moisture, and streamflow in the upper Feather River watershed due to vegetation changes postfire caused by the North Complex, Sugar, and Dixie Fires. The goals of this study were to quantify (1) long-term trends in climate and hydrology in the upper Feather River watershed, (2) postfire differences in water supply and other water balance variables using dynamic vegetation regrowth over three years in the upper Feather River watershed, and (3) whether the incorporation of postfire vegetation changes in the BCM improves streamflow accuracy.

2. Study area

The upper Feather River watershed in northern California is about 9300 km^2 and experiences some of the highest annual precipitation totals in the state, with an annual average of 1117 mm (Daly *et al* 2008). The precipitation distribution within the watershed has a unique pattern (figure 2(a)); the wettest part of the basin is confined to the western part of the watershed, where annual average precipitation can range from 1200 mm to more than 2000 mm (figure 2(a); Daly *et al* 2008). The northern and southeastern parts of the watershed receive, on average, less than 1000 mm of precipitation due to the rain shadow effect caused by the Sierra Nevada; the far southeastern corner receives less than 400 mm (figure 2(a); figure S1; Daly *et al* 2008). Most of the precipitation accumulates during October–March, but the runoff feeding into Lake Oroville comes from rain and snowmelt in January–June (Zamora-Reyes *et al* 2022). Recent studies have suggested that this region continues to experience increased precipitation and streamflow variability, complicating intra- and interannual management of water resources in the watershed (Swain *et al* 2018, Zamora-Reyes *et al* 2022). Annual water allocations from Lake Oroville through the SWP provide about 3.95 km^3 (3.2 million acre-feet (AF)) for drinking water and irrigation (California DWR 2025b), which is close to its total capacity of 4.19 km^3 (3.4 million AF).

The upper Feather River watershed is crucial to California's water supply; despite only making up 6% of the total area contributing flow to the Sacramento–San Joaquin Delta, it produces 14% of the outflow (California DWR and United States Bureau of Reclamation 2023). The watershed is divided into four subbasins: West Branch Feather River, North Fork Feather River, Middle Fork Feather River, and South Fork Feather River (figure 2). The North Fork Feather River comprises the largest area of the watershed and about 60% of the inflow into Lake Oroville while the Middle Fork Feather River contributes 30%, and the smaller West Branch Feather River and South Fork Feather River contribute just 5% (Koczot *et al* 2005, Walters *et al* 2024). This watershed is highly managed with powerhouses, diversions, and reservoirs that are used for several purposes in the watershed, such as hydropower, water supply, recreation, and flood control (Koczot *et al* 2005). This has resulted in altered discharge measurements at most stream-gaging stations in the region, making it difficult for modeling studies to use these data for calibrating a natural systems model (Walters *et al* 2024).

The upper Feather River watershed has a low population density and remains relatively undisturbed by human development. About 80% of the basin is managed by the United States Forest Service, and agricultural valleys on the eastern side are privately owned and used for hay production and livestock grazing (George *et al* 2007). There is a variety of vegetation types within the watershed, but the most common type is the Sierran mixed conifer (CALFIRE 2015), which covers about 42.2% of the basin and is an important part of the timber industry in the area (Koczot *et al* 2005; figure S2, table S1). Other dominant vegetation types include White fir (9.3%), Eastside pine (8.8%), sagebrush (5.7%), chaparral (5.6%), and grassland (3.5%; CALFIRE 2015; figure S2, table S1). The northeast and southwest areas of the basin are comprised of the Sierra Nevada and Basin and Range volcanic formations that allow deep percolation due to their high permeability, enhancing contributions toward groundwater flow (Koczot *et al* 2005). The central and southeastern parts of the watershed are made up of sedimentary and intrusive igneous formations, which tend to be less permeable than volcanic formations and contribute significantly to surface runoff, subsurface flow, and groundwater recharge (Koczot *et al* 2005).

3. Data and methods

3.1. BCM

The BCM (Flint *et al* 2021) is a monthly, gridded water balance model that calculates the water balance (precipitation minus ET minus sublimation minus runoff minus recharge minus change in storage is equal to zero) using climate inputs: precipitation, minimum temperature, maximum temperature, and potential ET (PET). Inputs, water balance equations, and the post-processing schematic are represented in the conceptual BCM diagram (figure 3). The upper Feather River BCM is a 30 m gridded model that was developed by spatially downscaling 4 km monthly Parameter-elevation Regressions on Independent Slopes Model (PRISM; https://prism.oregonstate.edu; Daly *et al* 2008) climate data (precipitation, minimum and maximum temperature) to 30 m (Flint and Flint 2012). The PET was calculated using air temperature and a modified Priestly–Taylor equation (Priestley and Taylor 1972, Flint and Childs 1991) together with topographic shading and cloudiness to calculate hourly PET. More detailed information about BCM calculations and pre-processing can be found in Flint *et al* (2021).

Static gridded model inputs include elevation, soil texture and thickness, land use, and geology. A 30 m digital elevation model was downloaded from The National Map (USGS 2022) and clipped to the upper Feather River watershed. The soil texture data (Batjes *et al* 2024), vegetation/land use (CALFIRE 2015), and geology (Horton *et al* 2017) were resampled to 30 m and clipped to the upper Feather River watershed.

A historical BCM run was used to calculate monthly water balance output variables from water years (WYs) 1896–2024. The hydrologic output variables derived by the BCM are (1) actual ET (AET), which is the water used by plants from soil storage; (2) climatic water deficit (CWD), which is the evaporative demand that exceeds available water (PET minus AET); (3) SWE, which is the previous month's accumulated snowpack plus the current snowfall minus the amount of water vapor lost to sublimation and snowmelt; (4) recharge, or the amount of water that makes it below the zone of ET to become baseflow or groundwater recharge; (5) runoff, or the excess water that can become streamflow; and (6) soil moisture storage, which is the total amount of water stored in the soil (precipitation plus snowmelt minus AET, recharge, and runoff). BCM variable units are millimeters per month, except for temperature, which is in degrees Celsius. Baseline AET outputs were calibrated locally to the upper Feather River watershed's dominant vegetation types (figure S2; tables S1 and S2), using gridded AET estimates from Reitz *et al* (2017) for October 2000 through September 2015. All model codes, control files, input and output layers, and the user's manual can be found in the 'Upper Feather River Watershed 30-meter Basin Characterization Model—Monthly Historical Climate and Hydrology' data release and model archive (Stern *et al* 2026). To further validate and qualitatively compare BCM estimates of ET, annual Moderate Resolution Imaging Spectroradiometer (MODIS) ET maps were downloaded from https://earthdata.nasa.gov/sensors/modis (Running *et al* 2021). Monthly BCM maps of AET were summed over each calendar year from 2020 to 2023 for comparison against the MODIS ET maps, but all other annual comparisons were done by WY (October through September).

Monthly streamflow data from 21 USGS (USGS 2024) and two California Data Exchange Center (CDEC 2024; https://cdec.water.ca.gov) stations were downloaded to calibrate simulated BCM streamflow from October 1896 to September 2024 (see table 1 for station details). Since many USGS stream gages in the watershed are affected by human alteration, only data from stations where diversion data were included and, in regions with dams or reservoirs, only pre-dam data were used (table 1). CDEC stations are full-natural flow estimates, which are a modeled representation of unimpaired streamflow

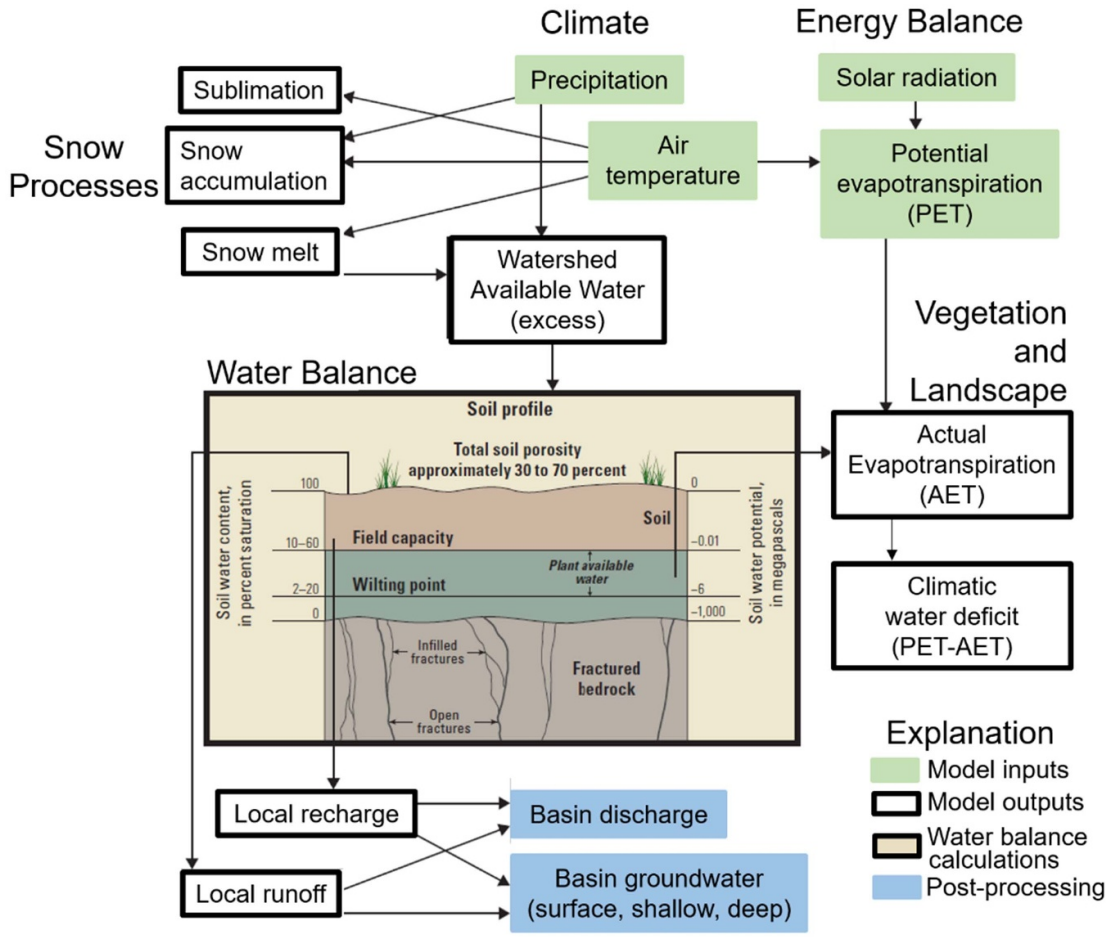


Figure 3. Schematic of the inputs and outputs and major water balance components within the BCM modified from Flint *et al* (2021).

calculated by the DWR (Huang and Kadir 2016). The period of record used was not consistent across all gages (table 1), and all available data were used for calibration with none for validation, as previous studies have suggested that it is not a necessary step in hydrologic modeling (table S3; Shen *et al* 2022). Simulated flows at each stream gage were post-processed using recharge and runoff output data that were summarized according to subbasin (see figure 4). Streamflow parameters were adjusted manually until the fit with measured data was optimized, and calibration goodness-of-fit statistics were maximized (table S3). The calibration statistics used included the coefficient of determination (R^2), the Nash–Sutcliffe coefficient of efficiency (NSE), and percent bias (PBIAS); these are standard metrics used to quantitatively compare observed and simulated flow (Stern *et al* 2016). To route upstream flow, individual subbasin flows were added to downstream subbasins. For more details about these methods, see the BCM techniques and methods report (Flint *et al* 2021).

3.2. Wildfire and vegetation index input

Thematic burn severity classification rasters derived from continuous normalized burn ratio images were downloaded from Monitoring Trends in Burn Severity (MTBS, https://mtbs.gov; Eidenshink *et al* 2007) for each wildfire at 30 m resolution. The burn severity maps were calculated using Landsat remote sensing data and categorized into six burn severity classes: unburned to low, low, moderate, high, increased greenness, and a non-processing mask (Eidenshink *et al* 2007). These rasters were then used to develop maps of vegetation change postfire as inputs to the BCM. Vegetation index maps (also called the LAI parameter in the BCM) used in the BCM represent an index of vegetation health and track vegetation growth and dieback through time as a function of climate variability (Flint *et al* 2021). The vegetation index maps are output from the BCM at a monthly time step and can be replaced to simulate vegetation disturbance (Flint *et al* 2021, 2024). To create vegetation index maps that accounted for changes in

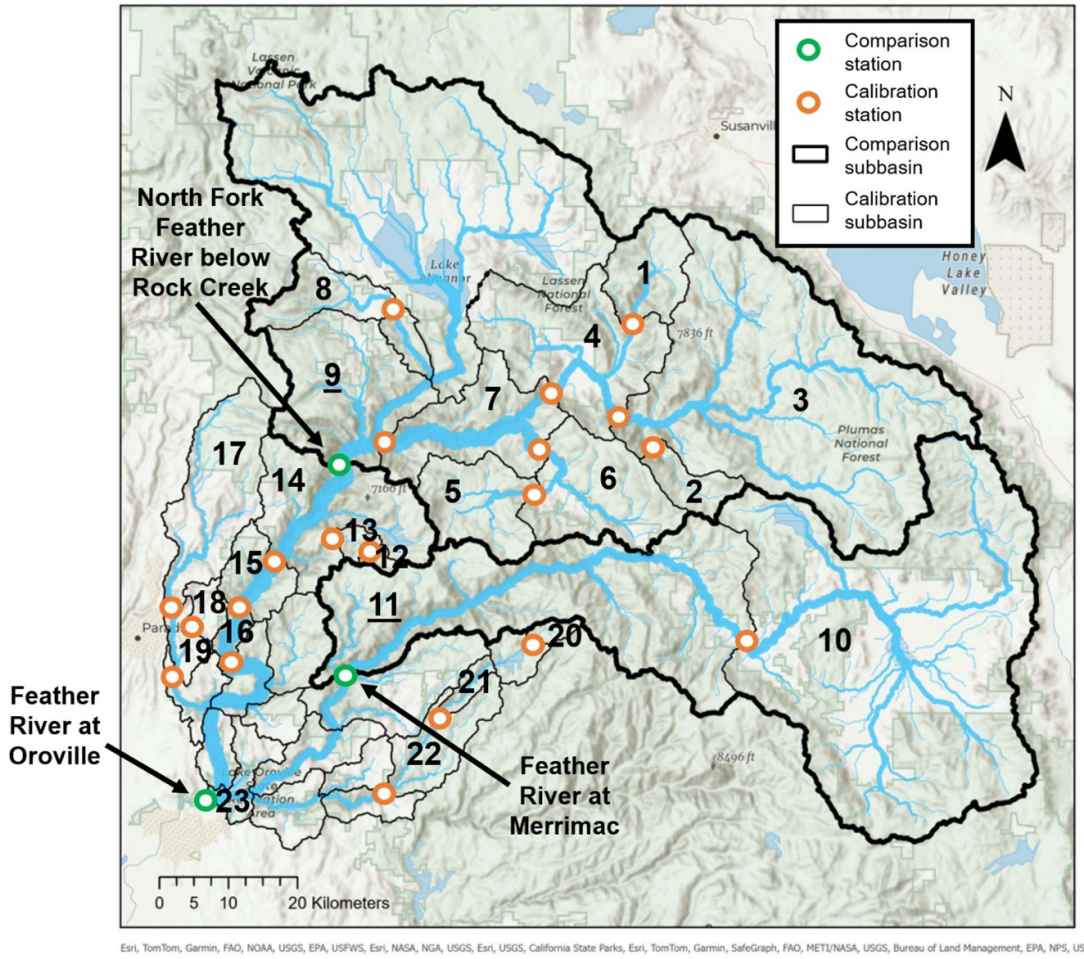


Figure 4. Upper Feather River watershed with streamflow calibration stations (orange circles) and their associated subbasins (thin black lines) used for model calibration (table 1), and the three comparison stations (green dots; underlined numbers, table 1) and their upstream subbasins (thick black lines) used to quantify changes in AET, soil moisture, and streamflow.

vegetation due to wildfires, each MTBS burn severity grid cell was replaced using the following conversions: unburned to low severity = 0.75, low severity = 0.50, moderate severity = 0.25, and high severity = 0.00 (Flint *et al* 2021). These new vegetation index maps were input into the BCM the month after the wildfire occurred to reduce vegetation density for the month postfire. After the burn severity-based vegetation index map was input, vegetation was allowed to grow and die back based on changes in climate, but no other BCM parameters were changed. The BCM uses a growth rate parameter that determines how quickly vegetation is allowed to grow back, based on the amount of precipitation received during a particular month relative to a long-term average (instead of average annual precipitation in normal mode; Flint *et al* 2021). In areas where the vegetation index is less than 1.00, the BCM reverts to a disturbance mode in which the vegetation parameters allow recovery of vegetation based on calibrated vegetation parameters to represent postfire regrowth (Flint *et al* 2021). Once the vegetation index returns to 1.00, normal vegetation calculations continue based on original vegetation type parameters. A baseline simulation with the same background climate data was run for the same period, except that it did not ingest the modified vegetation index maps; this simulation was used for a baseline (no fire) comparison.

Baseline and postfire AET, soil moisture, and streamflow were analyzed and compared for two stations and their contributing subbasins upstream as well as the full natural flow estimate at Feather River at Oroville (figure 4, green dots; bold stations in table 1). To quantify calibration changes due to model parameterization, baseline and postfire streamflow statistics were calculated separately for the baseline (2020–2024) and postfire (2020–2024) against measured and reference data (table 3). Percent differences of postfire to baseline at each streamflow station as well as runoff coefficients (annual streamflow divided by annual precipitation) were calculated to further understand the streamflow response to wildfires (table 4). Differences in baseline and postfire AET and soil moisture for three different groups were calculated using burned area thresholds within a subbasin (figure 4): subbasins with a total burned area

Table 1. Upper Feather River watershed calibration stations from the USGS and California DWR and associated subbasins used in this study (see figure 4 for locations).

Subbasin	Agency	Name of station	Station ID	Diversion station	Upstream area (km^2)	Period of record used
1	USGS	Lights Creek near Taylorsville	11 401 300	—	148	10/1957–09/1962
2	USGS	Little Grizzly Creek near Negesee	11 401 180	—	78	09/1964–09/1979
3	USGS	Indian Creek near Taylorsville	11 401 200	—	1366	10/1957–09/1980
4	USGS	Indian Creek near Crescent Mills	11 401 500	—	1913	10/1930–09/1993
5	USGS	Spanish Creek above Quincy	11 401 920	—	194	12/2009–09/2024
6	USGS	Spanish Creek above Blackhawk Creek at Keddie	11 402 000	—	476	10/1933–09/2024
7	USGS	East Branch North Fork Feather River near Rich Bar	11 403 000	—	2658	12/1967–09/1982
8	USGS	Butt Creek above Almanor	11 400 000	—	127	10/1936–09/1964
9	**USGS**	**North Fork Feather River below Rock Creek**	**11 403 200**	**11 403 800**	3193	**10/1986–09/2024**
10	USGS	Middle Fork Feather River near Clio	11 392 500	—	1777	10/1925–09/1979
11	**DWR**	**Feather River at Merrimac**	**MER**	**—**	2750	**11/1986–09/2024**
12	USGS	Grizzly Creek near Storrie	11 404 000	—	14	10/1929–09/1944
13	USGS	Grizzly Creek below Diversion Dam	11 404 300	11 403 700	37	10/1985–09/2024
14	USGS	North Fork Feather River below Grizzly Creek	11 404 330	11 404 360	372	10/1986–09/2000
15	USGS	North Fork Feather River at Pulga	11 404 500	—	468	04/1911–05/1958
16	USGS	North Fork Feather River above Big Bend	11 405 000	—	499	01/1906–12/1910
17	USGS	West Branch Feather River near Paradise	11 405 300	—	291	10/1957–09/1986
18	USGS	Concow Creek near Yankee Hill	11 406 000	—	39	10/1927–09/1952
19	USGS	West Feather River near Yankee Hill	11 406 500	—	377	10/1930–09/1963
20	USGS	South Fork Feather River above Little Grass Valley Reservoir	11 394 800	—	21	10/1960–09/1979
21	USGS	South Fork Tunnel near Strawberry Valley	11 395 150	11 395 200	97	10/1973–09/2006
22	USGS	South Fork Feather River below Forbestown Dam	11 396 200	11 396 290	227	10/1972–09/2010
23	**DWR**	**Feather River at Oroville**	**FTO**	**—**	9334	**10/1905–09/2024**

Stations used for comparison are in bold. Data summarized from USGS (2024) and CDEC (2024). FTO and MER are DWR station IDs for station #11 and #23, respectively.

<25%, subbasins with a total burned area >25% in the North Complex Fire in 2020 (table S4), and subbasins with a total burned area >25% in the Dixie and Sugar Fires in 2021 (table S5).

4. Results

4.1. Historical long-term climate and hydrology trends

The BCM was used to generate average annual (WYs 1991–2020) SWE (figure 2(b)), runoff (figure 5(a)), recharge (figure 5(b)), and runoff plus recharge (water supply; figure 5(c)). As expected, the average annual SWE in the upper Feather River watershed (figure 2(b)) follows a similar pattern to precipitation (figure 2(a)), where the highest amounts are in the western part of the basin and where elevations are the highest (figure S1). These areas accumulated more than 1000 mm in SWE, but the whole watershed (excluding low-lying elevations) received more than 50 mm of SWE on average, illustrating the importance of snow to the water supply (figure 2(b)). The highest average annual recharge and runoff patterns are similar to precipitation and SWE, except that most of the recharge and runoff is concentrated in the southwestern part of the upper Feather River watershed (figure 5). One notable difference between these two variables in this part of the basin is that average runoff tends to be higher in magnitude and covers a larger geographical area; the average annual runoff ranges from 600 to 1700 mm (figure 5(a)), while average annual recharge is mostly around 600 mm with some small areas reaching 1000 mm (figure 5(b)). These spatial patterns coincide with underlying bedrock permeability, where areas with volcanic formations and high permeability have the highest recharge, whereas those

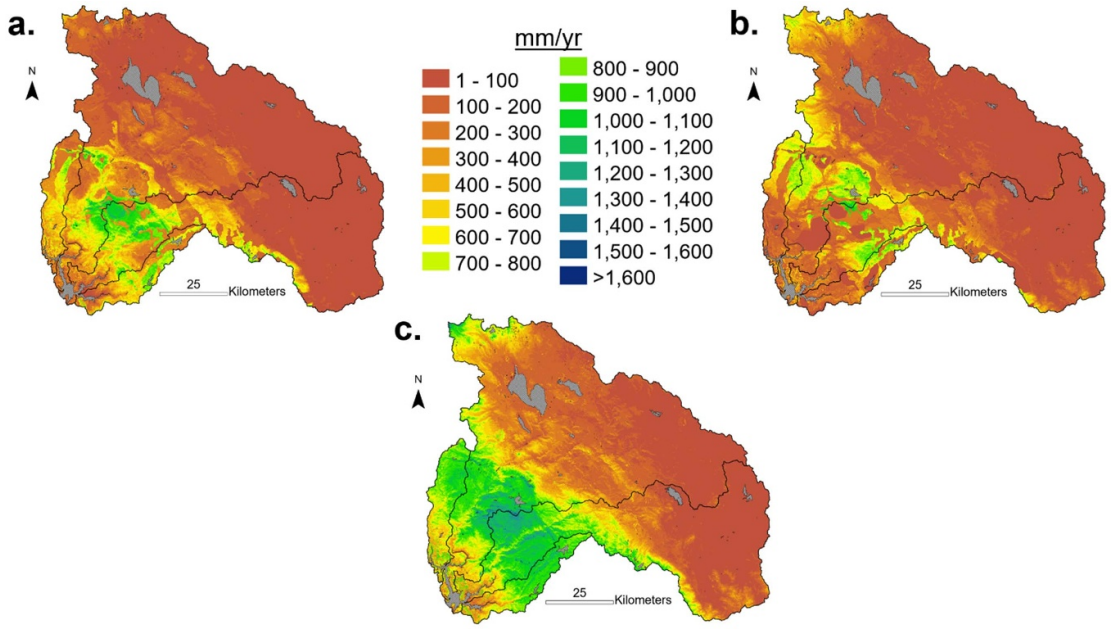


Figure 5. Average annual (a) runoff, (b) recharge, and (c) runoff plus recharge (water supply) modeled by the BCM (Flint *et al* 2021) for the upper Feather River watershed for WYs 1991–2020.

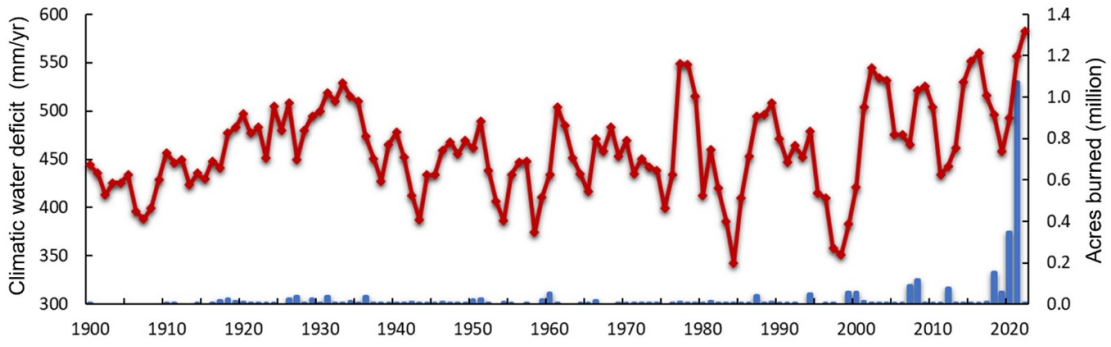


Figure 6. Three-year running average of the CWD from 1900 to 2023 for the upper Feather River watershed (red line) calculated by the BCM. Blue bars indicate the total acres burned in the watershed by calendar year from the California Department of Forest and Fire Protection's Fire and Resource Assessment Program dataset (CALFIRE 2015).

regions with intrusive igneous formations have lower permeability and higher runoff (Koczot *et al* 2005). Regardless of the breakdown between these two individual variables, the western area of the watershed has the highest water supply potential (figure 5(c)).

A three-year running average of the CWD or PET minus AET, a measure of water stress in the upper Feather River watershed, is shown in figure 6. The CWD has fluctuated since WY 1896 through dry and wet periods; however, the lowest and highest values were generated during the last 40 years. The CWD was less than 350 mm per year in 1984 and has been on a steady rise since 1999, attaining the highest value in 2023 (figure 6). This reflects the enhanced ability of the atmosphere to dry out vegetation as air temperatures continue to increase. The CWD appears to have become more variable over time, particularly after the mid-1970s (figure 6). Additionally, long-term average annual analysis of precipitation comparing values from 1981 to 2020 shows that the southwestern part of the upper Feather River watershed has experienced a decrease of up to 11 mm per year; in fact, most of the basin saw a decrease except for a minimal increase in the southeastern side of the basin (figure S3(a)). The same historical analysis comparing SWE values shows a more complex spatial pattern as higher elevations have experienced a 5–10 mm per year decrease, whereas low elevations showed minimal change (figure S3(b)).

4.2. Precipitation and SWE conditions before, during, and after wildfires

Spatial and temporal analyses of precipitation (figure 7) and SWE (figure S4) for WYs 2020–2024 revealed important context with respect to the long-term conditions described in section 4.1.

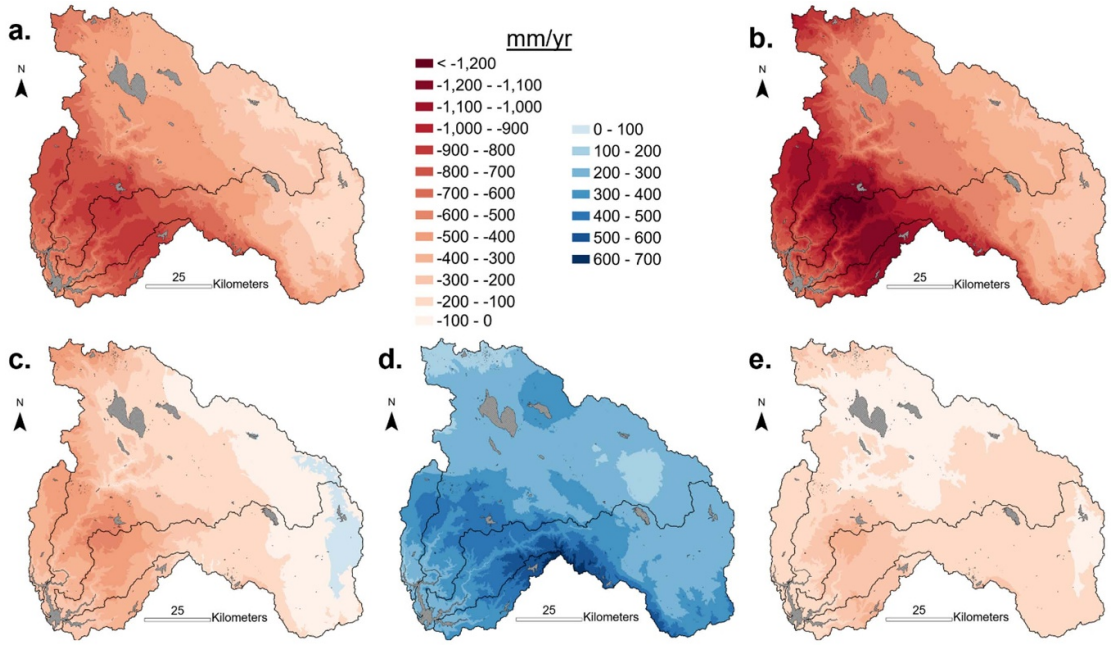


Figure 7. Average annual precipitation (1991–2020) subtracted from annual precipitation in WYs (a) 2020, (b) 2021, (c) 2022, (d) 2023, and (e) 2024 in millimeters per year for the upper Feather River watershed. These spatial maps were created using Daly *et al* 2008 data downscaled to 30 m grids.

During the winter of 2020, precipitation and SWE within the upper Feather River watershed were about 41.5% and 67.2% below the historical average from 1991 to 2020, respectively, leading up to the North Complex Fire during the summer of 2020 (figures 7(a) and S4(a)). These deficits were more pronounced the following year (2021) as precipitation dipped to 55.5% of the average (figure 7(b)), and the SWE was 86.6% of the average (figure S4(b)); the Sugar and Dixie Fires occurred a few months later in the summer and fall of 2021. WY 2022 provided little replenishment to the area; precipitation was about 82.2% of the average (figure 7(c)), and the SWE remained at very low levels at 13.9% of the average (figure S4(c)). After three years of consecutive dry conditions, the region saw a major surplus in precipitation (figure 7(d)) and SWE (figure S4(d)) in 2023; precipitation was 27.2% above the average while the SWE was 181.3% above the average. The last year included in this analysis (2024) had conditions that were closer to the long-term average: precipitation was slightly below the average (87.2%; figure 7(e)) while the SWE was slightly above the average (106.9%; figure S4(e)).

4.3. Postfire changes in AET, soil moisture, water supply, and streamflow

Modeled output from the two calibration stations—Feather River at Merrimac, which captures upstream changes caused by the North Complex Fire in 2020, and North Fork Feather River below Rock Creek, which captures upstream changes to the North Fork Feather River caused by the Sugar and Dixie Fires in 2021—showed decreases in AET (figure 8(a)) and increases in soil moisture (figure 8(b)) postfire.

The Feather River at Merrimac subbasin experienced changes in AET right after the North Complex Fire from the first through the fourth year postfire; the highest changes in AET occurred in the second year after the fire (figure 8(a), dotted lines). For the North Fork Feather River below Rock Creek subbasin, AET changes were seen immediately after the Sugar and Dixie Fires in 2021, but the most change occurred the year after, during the summer of 2022 (figure 8(a), solid lines). The average seasonal change in AET from WYs 2021 to 2024 in the Feather River at Merrimac subbasin decreased −9% (−3.2 mm) during fall (October–December), −10% (−6.6 mm) during winter (January–March), −11% (−26.5 mm) in spring (April–June), and −9% (−17.8 mm) in summer (July–September). The North Fork Feather River below Rock Creek resulted in higher decreases: −9% (−3.9 mm) during fall, −13% (−9.1 mm) in winter, −16% (−42.8 mm) in spring, and −16% (−38.5 mm) in summer. Maximum decreases in AET for both subbasins occurred during the summer of 2022 with −13% and −26% for the Feather River at Merrimac and North Fork Feather River below Rock Creek subbasins, respectively.

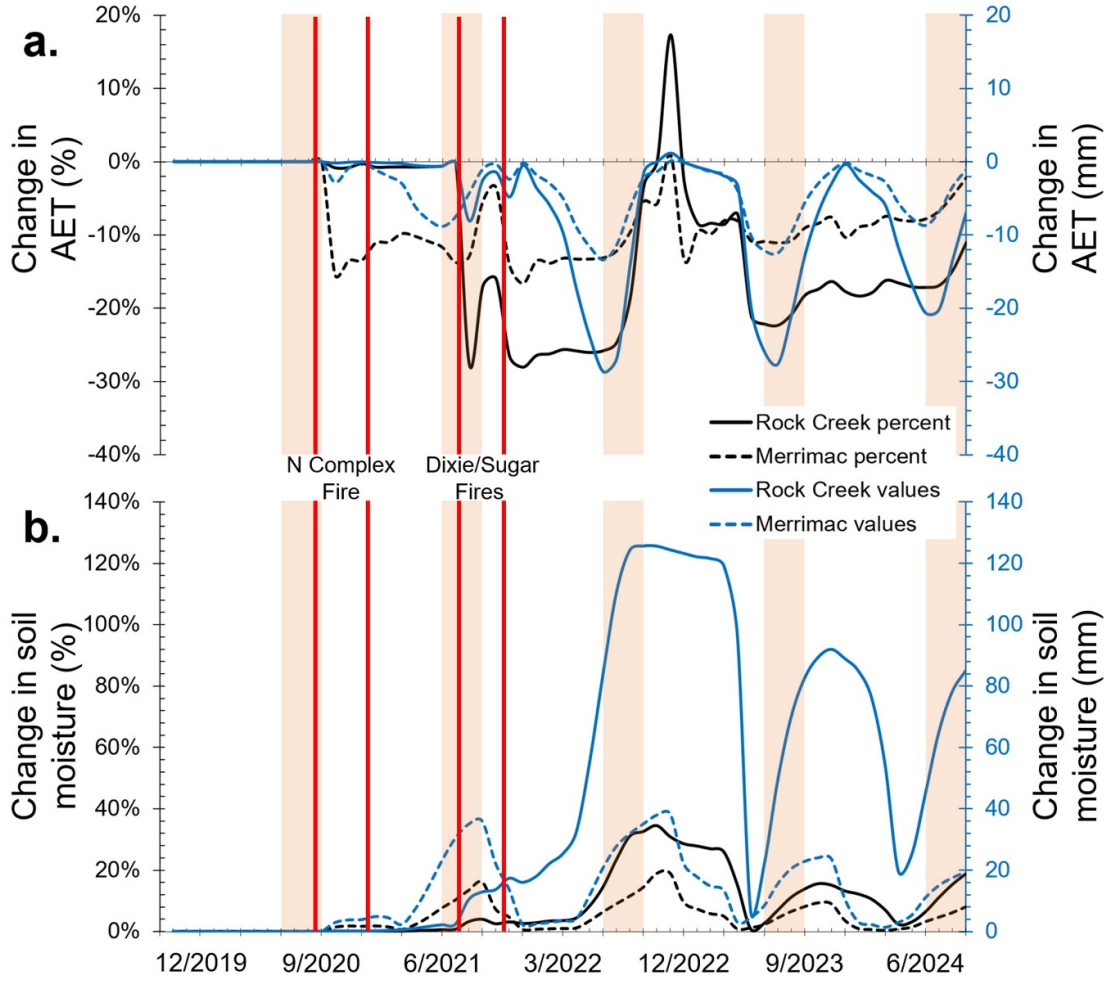


Figure 8. Simulated change in (a) AET and (b) soil moisture between postfire and baseline model runs for Feather River at Merrimac (Merrimac on the legend; dotted lines) and North Fork Feather River below Rock Creek (Rock Creek on the legend; solid lines) subbasins. Black lines show the relative change (difference between postfire and baseline with respect to baseline, in percent), and blue lines show the magnitude change (difference between postfire and baseline, in millimeters or mm). The start and end of the North Complex and Dixie and Sugar Fires are shown with vertical solid red lines; light orange shaded vertical rectangles denote June–August.

Increases in soil moisture changes were seen throughout the whole year, with the largest increases occurring between August and December 2022 (figure 8(b)). There was minimal change in soil moisture immediately following the fires, but the year after showed major increases for both subbasins, particularly for North Fork Feather River below Rock Creek (figure 8(b), solid lines). At Feather River at Merrimac, soil moisture differences were maximized two years postfire following the North Complex Fire (figure 8(b), dotted lines). The average seasonal change in soil moisture from WYs 2021 to 2024 in the Feather River at Merrimac subbasin increased from 7% (51.4 mm) during fall to 2% (18.3 mm) during winter, 3% (29.2 mm) in spring, and 9% (76.6 mm) in summer. For North Fork Feather River below Rock Creek, values were higher: 12% (172.9 mm) during fall, 10% (161.5 mm) in winter, 5% (97.9 mm) in spring, and 14% (203.9 mm) in summer. The maximum changes in seasonal soil moisture for both subbasins occurred during fall 2022 (16% or 98.5 mm and 31% or 373.4 mm). However, there were also large increases in winter 2023 for North Fork Feather River below Rock Creek (27% or 363 mm).

Changes in postfire AET and soil moisture led to changes in runoff plus recharge (water supply; figure 9). During WY 2021, water supply within the regions that burned in the upper Feather River watershed had a 25% increase compared to the baseline simulation, or an increase of about 2% of average (figure 9(a) and table 2). These increases continued through WY 2022 (figure 9(b)) and peaked during WY 2023 (figure 9(c)) when the postfire water supply increased 34% of average (table 2). In WY 2024, a close to average year with respect to precipitation and SWE, the postfire water supply continued to be above baseline (23% of average; table 2). Overall, the water supply after WY 2021 through WY 2024 showed an increased potential for streamflow generation within the North Complex and Sugar and Dixie Fire footprints.

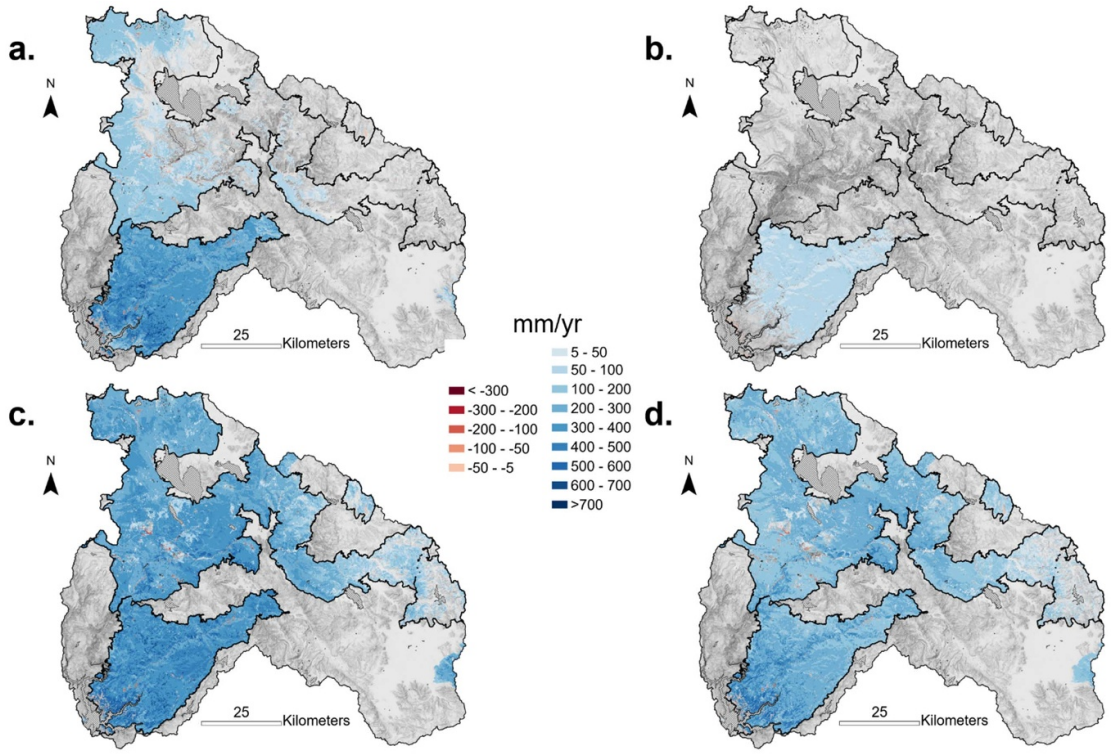


Figure 9. Average annual runoff plus recharge (water supply; 1991–2020) subtracted from annual precipitation for (a) 2021, (b) 2022, (c) 2023, and (d) 2024 in millimeters per year for the upper Feather River watershed. Recharge and runoff are modeled by the BCM (Flint *et al* 2021).

Table 2. Simulated annual postfire-to-baseline recharge plus runoff response in cubic meters (m^3) and AF within the upper Feather River watershed boundary.

	2021	2022	2023	2024
	m^3 (AF)	m^3 (AF)	m^3 (AF)	m^3 (AF)
Baseline	2.3×10^8 (186,827)	1.5×10^9 (1,215,393)	4.6×10^9 (3,720,502)	3.2×10^9 (2,557,402)
Postfire	2.9×10^8 (232,889)	2.0×10^9 (1,649,686)	5.8×10^9 (4,729,809)	4.0×10^9 (3,247,522)
Difference	5.7×10^7 (46,062)	5.4×10^8 (434,293)	1.2×10^9 (1,009,306)	8.5×10^8 (690,119)
Percent difference	24.7%	35.7%	27.1%	27.0%
Change relative to average year	1.6%	14.8%	34.3%	23.5%

Postfire streamflow resulted in higher values than baseline at Feather River at Merrimac, North Fork Feather River below Rock Creek, and Feather River at Oroville (figure 10). Immediately following the fires, there were only minimal differences between postfire and baseline after the North Complex Fire in Feather River at Merrimac (figure 10(a)) and the Sugar and Dixie Fires in North Fork Feather River below Rock Creek (figure 10(b)). The largest changes in streamflow occurred in December 2022 for Feather River at Merrimac (161% increase) and Feather River at Oroville (159% increase; figure 10(c)), whereas in North Fork Feather River below Rock Creek, the largest change occurred in March 2023 (101%). The average seasonal percent change in streamflow from WYs 2021 to 2024 in the Feather River at Merrimac subbasin ranged from 39% during fall to 19% during winter, 7% in spring, and 1% in summer. For North Fork Feather River below Rock Creek, increases were 11% during fall, 35% in winter, 18% in spring, and 13% in summer. Seasonal percent changes in streamflow for Feather River at Oroville were higher than baseline conditions: 39% during fall, 19% in winter, 10% in spring, and 5% in summer. The largest seasonal changes occurred during fall 2022 at Feather River at Merrimac (64%) and Feather River at Oroville (79%), while in North Fork Feather River below Rock Creek, this change occurred during winter 2023, two years postfire (73%; figure S5).

Overall, the incorporation of wildfire effects on vegetation into the BCM resulted in improved model streamflow statistics (table 3). All three stations showed increases in both monthly R^2 (between 0.04 and

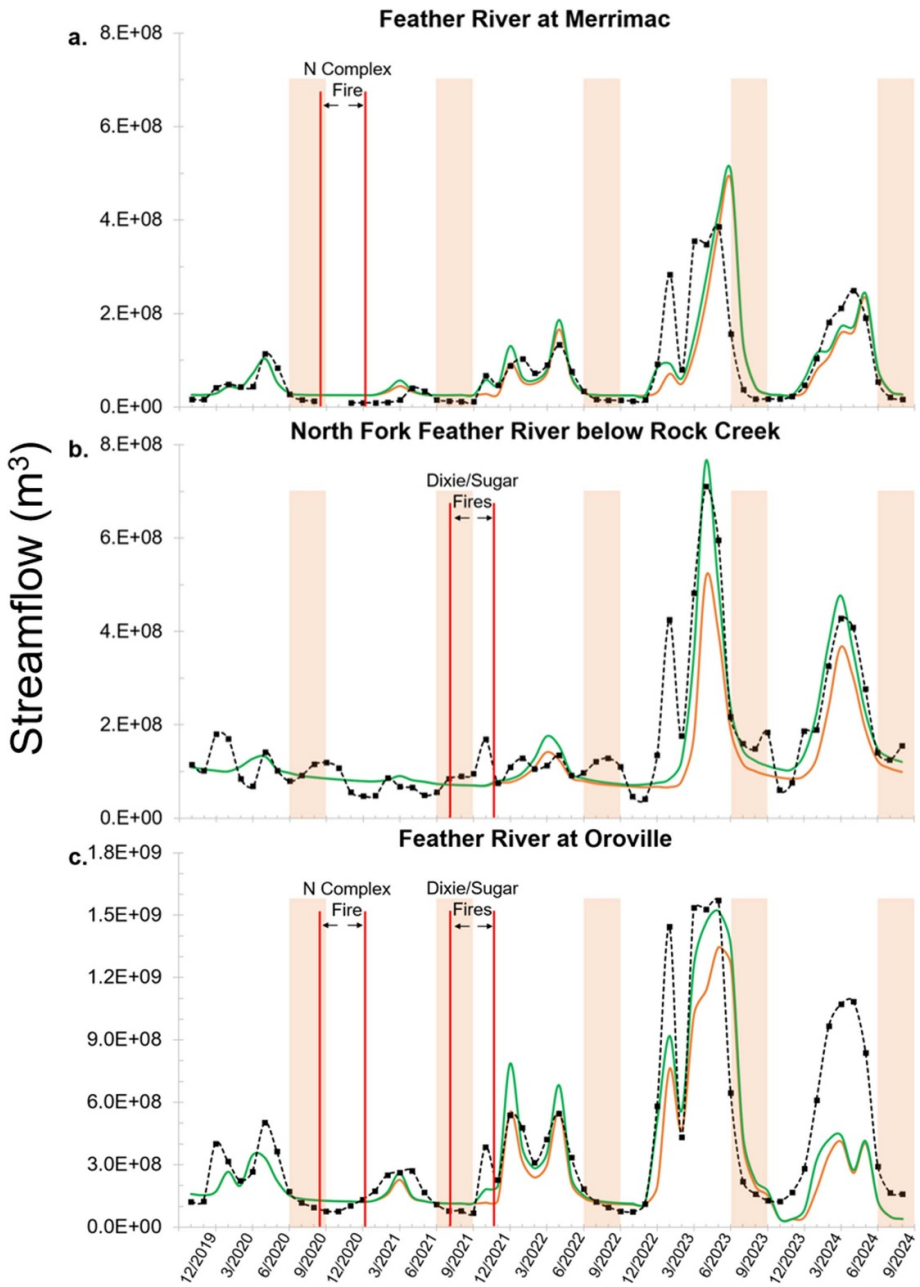


Figure 10. Simulated streamflow for baseline (orange line) and postfire (green line) for (a) Feather River at Merrimac, (b) North Fork Feather River below Rock Creek, and (c) Feather River at Oroville. The start and end of the North Complex and Dixie/Sugar Fires are shown with vertical solid red lines; light orange shaded vertical rectangles denote June–August. Monthly observed or reference data (see table 1 for details) are shown by black dotted lines.

0.07) and NSE (between 0.05 and 0.18) and decreases in PBIAS (between −2.7% and −15.2%). The percent difference of postfire-to-baseline annual streamflow was highest two years postfire for both subbasins: the Feather River at Merrimac annual flows increased by 20% in WY 2022, while North Fork Feather River below Rock Creek saw an increase of 37.1% in WY 2023 (table 4). Feather River at Oroville, which reflects changes accumulated over the whole watershed, saw increases in streamflow compared to baseline of 3.5% in WY 2021, 24.4% in WY 2022, 20.8% in WY 2023, and 16.2% in WY 2024 (table 4). The hydrologic response in all three streamflow stations postfire is captured in the runoff coefficient; this metric shows higher values from WY 2021 through WY 2024 postfire compared to baseline but particularly during the anomalous wet WY 2023 (table 4).

4.4. Postfire changes in AET and soil moisture by burn threshold

This study assessed the impact of wildfires on the water balance using a 25% threshold, where subbasins that were less than 25% burned were considered 'unburned' and those that were more than 25% burned

Table 3. Model statistics for baseline and postfire simulations including the coefficient of determination (R^2), NSE, and PBIAS. For locations, see figure 4, and for station details, see table 1.

	Feather River at Merrimac				North Fork Feather River below Rock Creek				Feather River at Oroville			
	Calibrated baseline	Baseline (2020–2024)	Postfire (2020–2024)	Difference	Calibrated baseline	Baseline (2020–2024)	Postfire (2020–2024)	Difference	Calibrated baseline	Baseline (2020–2024)	Postfire (2020–2024)	Difference
Measured flow (m^3)	—	4.33×10^9		—	—	9.46×10^9		—	—	2.26×10^{10}		—
BCM flow (m^3)	—	4.08×10^9	4.56×10^9	12.0%	—	7.02×10^9	8.46×10^9	20.5%	—	1.60×10^{10}	1.86×10^{10}	16.1%
Monthly R^2	0.64	0.50	0.56	0.06	0.57	0.72	0.79	0.07	0.81	0.66	0.70	0.04
NSE	0.62	0.45	0.50	0.05	0.51	0.59	0.77	0.18	0.81	0.59	0.68	0.09
PBIAS	0.0%	7.0%	4.3%	−2.7%	0.0%	25.8%	10.5%	−15.2%	0.0%	29.1%	17.7%	−11.4%

Table 4. Simulated annual postfire-to-baseline watershed response in comparison streamflow stations. The runoff coefficient (discharge/precipitation) for each station is also shown. For station details, see figure 4 and table 1. Stations used for comparison in the results are in bold.

		Feather River at Merrimac				North Fork Feather River below Rock Creek				Feather River at Oroville			
		2021	**2022**	**2023**	**2024**	**2021**	**2022**	**2023**	**2024**	**2021**	**2022**	**2023**	**2024**
Upstream area (km^2)		2750				4587				9334			
Annual precipitation (mm)		433	858	1327	835	442	790	1216	849	497	919	1420	974
Annual streamflow (m^3)	Baseline	3.2×10^8	6.0×10^8	1.4×10^9	8.5×10^8	8.5×10^8	1.0×10^9	2.1×10^9	1.8×10^9	1.5×10^9	2.6×10^9	6.4×10^9	2×10^9
	Postfire	3.4×10^8	7.1×10^8	1.6×10^9	9.5×10^8	8.5×10^8	1.1×10^9	3.0×10^9	2.5×10^9	1.5×10^9	3.1×10^9	7.9×10^9	2×10^9
Percent difference		**4.9%**	**18.5%**	**13.6%**	**11.5%**	**0.0%**	**11.1%**	**43.6%**	**35.7%**	**3.1%**	**19.0%**	**22.8%**	**14.9%**
Runoff coefficient	Baseline	0.27	0.25	0.39	0.37	0.42	0.28	0.38	0.46	0.32	0.31	0.48	0.21
	Postfire	0.29	0.30	0.45	0.41	0.42	0.31	0.54	0.63	0.33	0.37	0.59	0.24

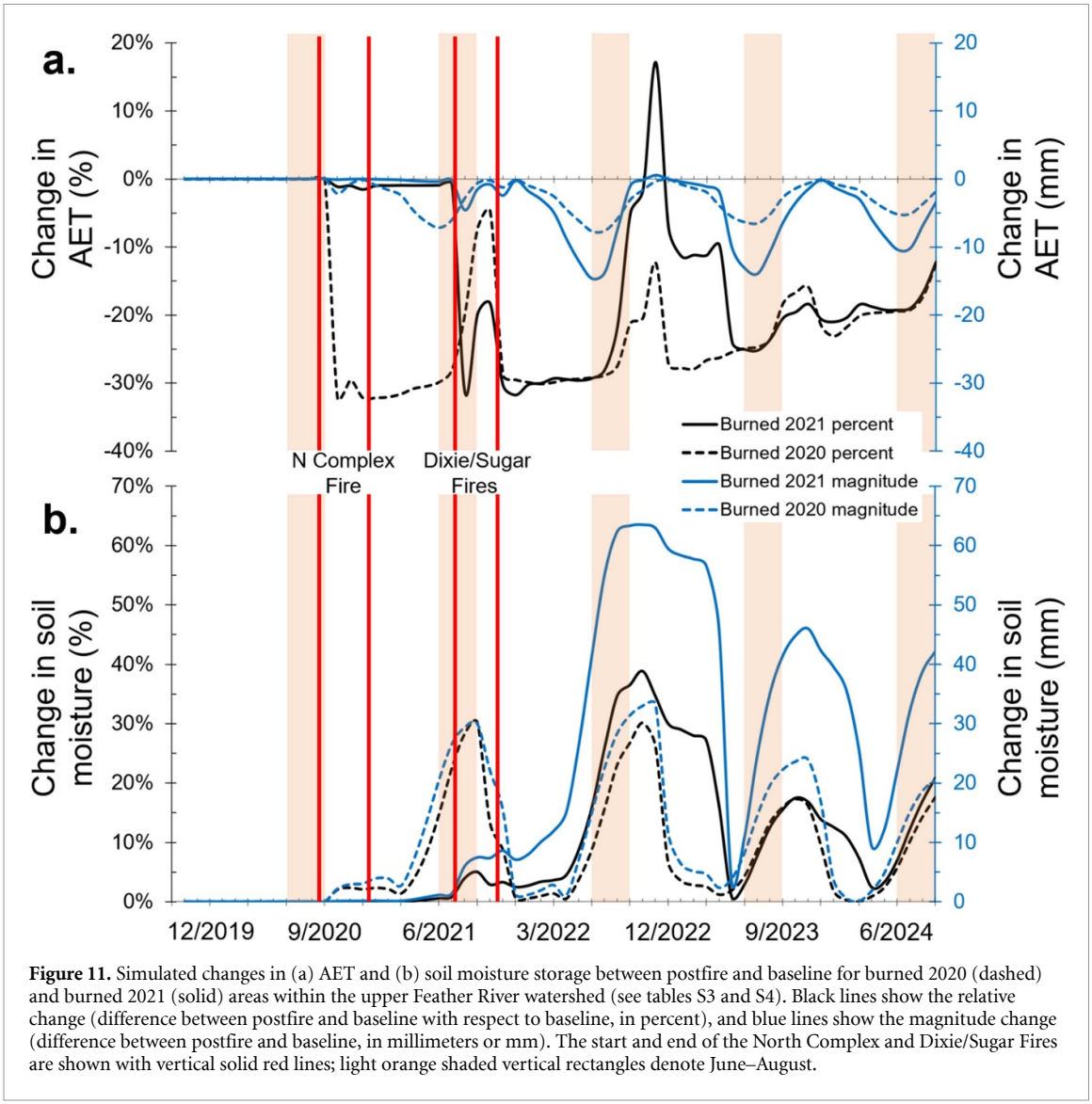


Figure 11. Simulated changes in (a) AET and (b) soil moisture storage between postfire and baseline for burned 2020 (dashed) and burned 2021 (solid) areas within the upper Feather River watershed (see tables S3 and S4). Black lines show the relative change (difference between postfire and baseline with respect to baseline, in percent), and blue lines show the magnitude change (difference between postfire and baseline, in millimeters or mm). The start and end of the North Complex and Dixie/Sugar Fires are shown with vertical solid red lines; light orange shaded vertical rectangles denote June–August.

were considered 'burned,' and separated by burn year (2020 or 2021; tables S4 and S5). The separation of these subbasins into unburned or burned resulted in similar patterns to the analysis focused on total upstream areas from the Feather River at Merrimac and North Fork Feather River below Rock Creek gages, where decreases to AET (figure 11(a)) and increases to soil moisture (figure 11(b)) were captured postfire.

The difference from baseline for AET after the North Complex Fire (figure 11(a), dashed lines) and after the Sugar and Dixie Fires (figure 11(a), solid lines) showed the highest change after the first and second years postfire (about −30% or −7 mm for areas burned in 2020 and almost −32% or −15 mm for areas burned in 2021) while the unburned areas (figure S6(a)) showed minimal differences compared to baseline. The average seasonal change in AET from WYs 2021 to 2024 for the subbasins burned in 2020 saw values of 21% (−2.2 mm) during fall, −28% (−4.5 mm) in winter, 26% (−16.4 mm) in spring, and 22% (−12.7 mm) in summer. For subbasins burned in 2021, the average seasonal change for fall was −11% (−2.1 mm), −15% (−4.2 mm) in winter, 18% (−21.8 mm) in spring, and −20% (−19.5 mm) in summer. On an annual basis, the baseline-to-postfire change in AET for the combined annual averages of subbasins burned in 2020 and 2021 was −16% (−5.4 mm) in WY 2021, −26% (−14.1 mm) in WY 2022, −19% (−11.8 mm) in WY 2023, and −19% (−10.7 mm) in WY 2024.

There were minor changes in soil moisture immediately postfire in areas burned in 2020 (figure 11(b), dashed lines) and 2021 (figure 11(b), solid lines). Soil moisture changes peaked during the fall of 2022, when both burned areas had major increases above 30% or more than 35 mm for areas burned in 2020 and close to 70 mm for areas burned in 2021 (figure 11(b)), while unburned areas remained relatively unchanged (figure S6(b)). The average seasonal change in soil moisture from WYs

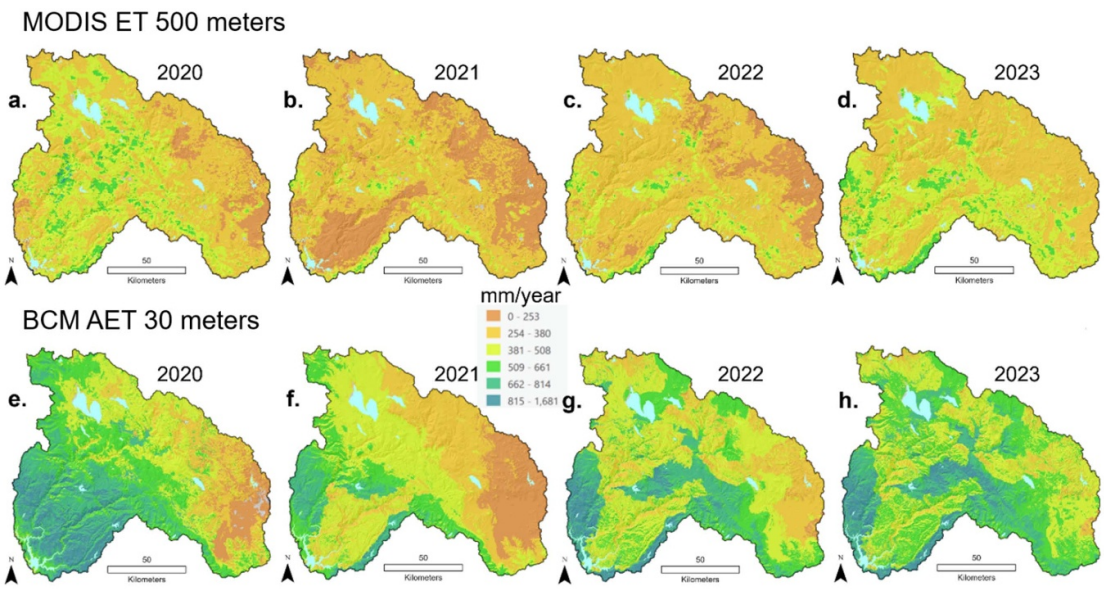


Figure 12. Calendar year total (a)–(d) MODIS ET (Running *et al* 2021) and (e)–(h) BCM (Flint *et al* 2021) simulated AET in mm per year.

2021 to 2024 in the unburned areas ranged from 3% (15.6 mm) during fall to 2% (14.5 mm) in winter, 2% (13.9 mm) in spring, and 4% (21.8 mm) in summer. Areas burned in 2020 saw higher values: 11% (47.4 mm) during fall, 2% (9.3 mm) in winter, 5% (23.8 mm) in spring, and 19% (69.7 mm) in summer, while the highest average seasonal values were found in areas burned in 2021: 13% (85.6 mm) during fall, 10% (76 mm) in winter, 5% (47.3 mm) in spring, and 16% (102.3 mm) in summer. On an annual basis, the baseline-to-postfire change in soil moisture for the combined annual averages of subbasins burned in 2020 and 2021 was 5% (20.4 mm) in WY 2021, 10% (58.4 mm) in WY 2022, 15% (85.6 mm) in WY 2023, and 10% (66.3 mm) in WY 2024.

The wildfire footprints within the upper Feather River watershed differed between 2020 and 2021; the North Complex Fire burned about 1162 km^2, while the Sugar and Dixie Fires burned 3014 km^2, or more than double the North Complex Fire. Another difference between these fires is that the North Complex Fire was of higher severity than the Sugar and Dixie Fires, as the majority of the subbasins had a moderate to high severity burn (tables S4 and S5). The most common vegetation types that burned during the North Complex and Sugar/Dixie Fires were Sierran mixed conifer (42% and 51%, respectively) and white fir (15% and 9%, respectively), which are similar to the overall vegetation composition of the upper Feather River watershed (table S1). One difference between the vegetation types burned during the two fires is that the North Complex Fire had a higher percentage of burned area of montane hardwood and montane hardwood-conifer (almost 24% compared to less than 4% for the Sugar/Dixie Fires; table S1); this type of vegetation has higher water use than Sierran mixed conifer and white fir (Flint *et al* 2024).

4.5. Comparison of ET between MODIS and BCM

MODIS ET (500 m resolution) data were used for qualitative validation and comparison to the BCM AET (30 m resolution) output and showed that, in general, the BCM AET tended to be higher than MODIS for WYs 2020–2023 (figures 12 and S7). This difference is more acute in 2022, where the average MODIS ET was 477.9 mm and 511.9 mm for the BCM (figures 12(c), (g), and S7(b)). The lowest ET values for MODIS and the BCM occurred in 2021 (445.3 mm and 412.2 mm; figure S7(b)) while the highest ET values occurred in 2023 (538.2 mm and 563.3 mm; figure S7(b)). The footprints of the North Complex and Dixie Fires were visible in both ET results, but the MODIS ET showed a faster recovery of AET by WY 2023 compared to BCM AET estimates.

5. Discussion

This multi-year process-based modeling study reveals that the water balance within the upper Feather River watershed has undergone major changes since summer 2020 due to the impact of some of the

largest wildfires in California's history, which have a combined burn area of 4800 km^2 or 480 000 hectares, equaling more than half of the basin. The study used two streamflow stations for comparison: Feather River at Merrimac, which represents changes to the Middle Fork of the Feather River watershed, and the North Fork Feather River below Rock Creek, which represents changes to the largest contributor of streamflow to Lake Oroville, the North Fork of the Feather River. The Feather River at Merrimac was predominantly affected by the North Complex Fire, and the North Fork Feather River below Rock Creek gage was mostly affected by the Dixie and Sugar Fires. Both subbasins showed increases in AET and soil moisture compared to baseline conditions directly after the fires occurred, but most of the change occurred in the spring and summer for AET and fall, winter, and summer for soil moisture one to four years postfire (figure 8). A similar pattern in streamflow, where differences were maximized during the fall, continued throughout the winter and spring, and minimized by summer, was also shown (figures 10 and S5). This is consistent with other studies in the Sierra Nevada that have shown postfire increases in spring snowmelt streamflow with lesser changes in summer baseflow (Boisramé *et al* 2019). Although these results indicate a decrease in ET that results in higher streamflow and baseflow similar to a recent study in the western United States (Williams *et al* 2022, Furniss *et al* 2025), other studies have found that wildfires can reduce late-season streamflow via reduced snowpack retention (Kampf *et al* 2022, Koshkin *et al* 2022) or increased ET from rapid postdisturbance growth or increased evaporation (Goeking and Tarboton 2020). While the upper Feather River watershed may have begun to slowly recover from these wildfires (figure 12), it might be years to decades until it returns to pre-fire conditions (Blount *et al* 2020, Niemeyer *et al* 2020), especially in high burn severity areas. Moreover, this relatively unmanaged watershed may not return to pre-fire conditions when vegetation was burned with high severity and therefore may continue to experience decreased AET and increased soil moisture and streamflow into the future (Kinoshita and Hogue 2011, Ma *et al* 2020, Niemeyer *et al* 2020, Williams *et al* 2022, Wells *et al* 2024).

The period between December 2022 and March 2023 was one of the wettest on record in California (figure 7(d)) and occurred after an intense dry period from 2020 through 2022 (figures 7(a)–(c)). This region received an average precipitation of 1420 mm during WY 2023 (127% of average), while WYs 2020, 2021, 2022, and 2024 received much less with 653 mm (58% of average), 497 mm (48% of average), 919 mm (82% of average), and 974 mm (87% of average), respectively. SWE, an important measure of how much water is stored as snowpack for use during the dry season, followed a similar pattern during these five years (figure S4). These extreme climatic conditions are reflected in the high CWD experienced in the upper Feather River watershed leading up to the North Complex, Sugar, and Dixie Fires (figure 6). The increased precipitation conditions in WY 2023 throughout the basin led to the saturation of soils in the area, which were also experiencing lower AET due to postfire changes in vegetation cover. During this same period, postfire AET was lower than the baseline, suggesting that the vegetation had not returned to pre-fire conditions (Niemeyer *et al* 2020).

The combined effects of decreased vegetation after the North Complex, Sugar, and Dixie Fires, plus record precipitation during the WY 2023 season, led to increased water supply potential in areas located within the wildfire footprint (figure 9(c)), and further analysis suggested higher streamflow magnitudes postfire at all three comparison locations, particularly in the North Fork Feather River below Rock Creek and the outlet station, Feather River at Oroville (figures 10(b) and (c)). The inclusion of vegetation changes due to wildfires within the watershed resulted in a water supply surplus of 1.2 km^3 in WY 2023 alone (1 million AF; table 2), which equates to almost a third of Lake Oroville's capacity, and led to an increase of 21% more streamflow in the upper Feather River basin that year (table 4). Such 'savings' continued into WY 2024, where the surplus in the water supply was 8.5×10^8 m^3 or 0.8 km^3 (690 000 AF; table 2) and about 16% more streamflow into Lake Oroville (Feather River at Oroville; table 4). It is hard to separate the individual contribution between the wildfires and the extraordinary precipitation in the WY 2023 season as it has become more difficult to assess and model an 'average' winter in California due to the high hydroclimatic variability in the region (Zamora-Reyes *et al* 2022). However, in the western United States, this relationship becomes non-linear (Williams *et al* 2022) and could be further studied in this watershed. Previous efforts to quantify water balance dynamics postfire in the upper Feather River watershed relied on remote sensing only and did not analyze streamflow data due to the highly managed system (Walters *et al* 2024), missing an important element toward a more comprehensive understanding of hydrological processes in the region. As precipitation variability throughout the state continues to increase into the 21st century, it is important for future studies to focus on improving the understanding of the relationship between extreme precipitation events (Swain *et al* 2018, Zamora-Reyes *et al* 2022, Touma *et al* 2022) and the long-term effects of the North Complex and Dixie Fires on runoff, soil moisture, and AET in the upper Feather River watershed.

Previous studies have indicated possible wildfire burn thresholds at which changes in postfire vegetation coverage and intensity are significant enough to produce changes in the water balance (Saxe *et al* 2018). Although there is some consensus in the literature of a 20% wildfire burn threshold within a watershed to see major hydrologic change (Hallema *et al* 2018, Saxe *et al* 2018, Wine *et al* 2018, Williams *et al* 2022), this study used a threshold of 25% or more burned area, since there was very little change between baseline and postfire model runs between unburned areas (25% or less burned area) and those that burned (greater than 25% burned area) during 2020 and 2021 (figure S6 vs. figure 11). The results reinforced the idea that there was not enough of a disturbance to see significant changes within those basins below the threshold. For the basins that exceeded this threshold, changes in AET and soil moisture were highest in the second year postfire (figure 11) and may likely continue to impact water resources into the future due to the size and severity of the North Complex and Dixie Fires that burned over half of the watershed. Across the upper Feather River watershed, 29% was moderately burned, and 31% was severely burned. Studies in adjacent watersheds, the Yuba River and American River, which have similar vegetation to the upper Feather River watershed, examined wildfires between 1985 and 2018 and found that medium-intensity wildfires (defined in Roche *et al* 2020 as those with a loss in basal area between 25% and 75%) in that period did not have a significant effect on streamflow even though they caused large ET changes due to vegetation cover reduction, which could also be explained by the size of the wildfires relative to the size of the watershed (Roche *et al* 2020). The largest wildfire included in that study was 8% of the watershed (the American River watershed area is 4825 km^2, and the King Fire in 2014 burned 373 km^2 of the watershed; Roche *et al* 2020), which is much smaller than the North Complex or Dixie Fires and the 25% threshold. Thus, the upper Feather River watershed and the wildfires of 2020 and 2021 are a unique case study in postfire hydrology due to the combined effects of the watershed size and the percent of burned area, as no other studies of comparable watershed or wildfire size were found at the time of writing this paper.

This study highlights the flexibility of the BCM for investigating hydrological changes due to disturbances such as wildfires that may be difficult to directly measure. One of the major advantages of this model is its ability to incorporate bedrock conductivity, an often-ignored variable in rainfall-runoff models, which can lead to better recharge and runoff estimates (Flint *et al* 2021, 2024). The BCM integrates vegetation parameters, such as growth rates and vegetation health, that have been calibrated for 72 different vegetation types in California; it should be noted that the baseline BCM version does not include any of the wildfire effects. A recent literature review suggested that it is important to incorporate vegetation growth and health in postfire modeling studies to better understand associated hydrologic changes (Ebel *et al* 2023). Others have argued that physically based models will become increasingly important to understand hydrological processes postfire (Partington *et al* 2022) and that future studies on postfire processes should include the ability to quantify at least annual precipitation, annual maximum SWE, and the magnitude of hydrologic change (Goeking and Tarboton 2020).

Water balance models are powerful investigative tools that can be used to simulate historical and future hydrological changes due to climate and land use, yet they have inherent limitations that should be considered when interpreting results from this study. The BCM simulates snowpack processes using the SNOW-17 model, which does not have the capability to model snow interception or vegetation impacts on snow attenuation (Anderson 2006). Although snowpack was calibrated to snow pillow and snow course data across California (CDEC 2024), this model assumption may lead to higher uncertainty in snow accumulation and melt processes and the seasonality of snowpack. The BCM is an unimpaired watershed model, which means human-induced changes like diversions, urbanization, logging, and other disturbances are not explicitly modeled. The BCM does not include streamflow routing directly, as streamflow is calculated using a postprocessing spreadsheet that accumulates recharge and runoff for all grid cells upstream of a gage location (Flint *et al* 2021). This may be a limitation if there are significant surface water–groundwater interactions above and below the gage location or if ungaged diversion data are not available. In addition, lateral flows are not simulated, which may or may not be a large source of uncertainty depending on local soil and topographic and geologic conditions. The BCM also does not simulate loss of surface cover, soil sealing, ash layers, or hydrophobicity (where soil particles are sometimes affected by wildfire to repel water), which affect runoff generation. Many studies have shown that soil conditions may be hydrophobic before wildfires, that hydrophobicity is non-continuous across a landscape, or that soils may become hydrophobic postfire. Therefore, the runoff processes may be enhanced or reduced, depending on the local soil properties and soil burn severity, adding to the uncertainty of the projected changes in streamflow. Without additional soil data, it is not possible to accurately characterize the soil hydrophobicity or soil sealing across the watershed, and in this study, the soil conditions were assumed to be the same pre- and postfire.

Another limitation to this study is the lack of measured ET and soil moisture data to validate BCM outputs. However, the comparison between the MODIS ET and the BCM AET showed that BCM post-fire simulations captured the changes in ET due to the 2020 and 2021 wildfires (figure 12). The BCM annual ET was higher compared to MODIS (figure S7), yet previous studies have suggested that MODIS generally underestimates ET (Mu *et al* 2011). Previous wildfire footprints, including the Walker Fire in 2019 and the Camp Fire in 2018, were visible in the MODIS ET and likely affected watershed processes but were not covered in this study since they occurred before 2020. Future work could incorporate all major recent fires including the Camp and Walker Fires and several smaller fires that occurred over the last ten years in the watershed. Very few studies have evaluated soil moisture model performance against instrumental data or used it for initial conditions (Ebel *et al* 2023), and more soil moisture data could help to fill this information gap in this watershed. Incorporating additional soil moisture data may help calibrate the model to improve the understanding of drying and wetting cycles in a snow-dominated location and the current understanding of high runoff production areas throughout the watershed. The BCM's vegetation growth parameters could also be calibrated against soil moisture instrumental data to incorporate subsequent adjustments to the vegetation caused by climatic variation that may not be adequately represented by the fire effects. Further work could also address vegetation type conversion, which is not accounted for in this study. Insight into these processes is critically important for water resource management and streamflow forecasting.

6. Conclusions

The cascading impacts of wet and dry extreme climatic events in California, such as droughts, floods, and wildfires, are directly affecting the state's water supply. This study was the first to quantify the changes to the monthly, seasonal, and annual AET, soil moisture, and streamflow changes in the upper Feather River watershed following the North Complex Fire in 2020 and the Dixie and Sugar Fires of 2021 using a process-based model. This study used the BCM, a gridded water balance model, which allowed for the dynamic integration of vegetation change resulting from the wildfires. The combined effects of decreased AET after the North Complex, Sugar, and Dixie Fires with record precipitation during the WY 2023 season led to enhanced soil moisture levels and higher streamflow postfire at all three streamflow stations used in the study; the upper Feather River basin saw 32% higher streamflow during WY 2023 and 16% in WY 2024. Although the majority of this change occurred during the wet season, its effects were evident during the dry season as increases to summer baseflow of 12% in WY 2023 and 2% in WY 2024.

These results are important for local, state, and federal agencies that monitor and manage the water supply in the state to consider since relatively unmanaged basins affected by intense wildfire, such as the upper Feather River watershed, are likely to continue to experience above normal streamflow due to vegetation changes for years to decades (Blount *et al* 2020, Niemeyer *et al* 2020). Studies have shown that forest thinning and controlled burns are promising methods for enhancing water supply resilience (Robles *et al* 2014, Sun *et al* 2015, Boisramé *et al* 2017, Loverin *et al* 2024). There may be a buffering effect to this level of disturbance on the watershed, and other studies have shown there are potential benefits of managing forests to maintain water supply resilience (Sun *et al* 2015, Boisramé *et al* 2017, Niemeyer *et al* 2020). However, a generic approach to forest management for water supply can cause unintended consequences, such as increasing forest water use and drought vulnerability (Tague *et al* 2019).

Although the results presented in this paper indicate that wildfires may benefit the water supply, predictions of increased precipitation variability throughout California can leave the state in a more vulnerable situation that may require flexible adaptation strategies to reduce flood risk (Swain *et al* 2018, Touma *et al* 2022, Zamora-Reyes *et al* 2022). Future work could include additional validation of BCM soil moisture outputs in the upper Feather River watershed against *in situ* soil moisture and ET data to improve the understanding of runoff generation in the region. Studies have suggested continued management of mixed-conifer forested lands in upstream watersheds that supply water to sustain these water benefits and are likely to become increasingly important through climate change, disturbances like wildfire and landslides, and other land use changes (Boisramé *et al* 2019). The upper Feather River watershed is one important piece of the complex water system in California that could benefit from a coordinated effort between several agencies across the state to manage resources for wildlife, municipal and residential water supply, and agricultural use into the future.

Acknowledgment

This work was funded by the California Department of Water Resources under Agreement No. 4600014343. We want to thank Brian Ebel and the three anonymous reviewers for all their comments and suggestions, which greatly helped to improve this manuscript.

Data availability statement

All model codes, control files, input and output layers, and the user's manual are available on the 'Upper Feather River Watershed 30-meter Basin Characterization Model—Monthly Historical Climate and Hydrology' data release and model archive (Stern *et al* 2026). Streamflow data for USGS stations can be found on the USGS Water Data for the Nation website (https://waterdata.usgs.gov; USGS 2024) and for the California DWR stations on the CDEC website (https://cdec.water.ca.gov; CDEC 2024). MODIS ET data are available on the MODIS website (https://earthdata.nasa.gov/sensors/modis; Running *et al* 2021). Burn severity classification rasters can be downloaded from the MTBS website (https://mtbs.gov; Eidenshink *et al* 2007).

The data that support the findings of this study are openly available at the following URL/DOI: https://doi.org/10.5066/P138MUCW.

Supplementary data 1 available at https://doi.org/10.1088/2752-5295/aea9bf/data1.

Conflict of interest

There is no conflict of interest for any of the authors. Any use of trade, firm, or product names is for descriptive purposes only and does not imply endorsement by the US government.

Author contributions

Diana Zamora-Reyes 0000-0001-6982-9413
Conceptualization (equal), Data curation (equal), Formal analysis (lead), Investigation (lead), Methodology (equal), Project administration (lead), Validation (lead), Visualization (lead), Writing – original draft (lead), Writing – review & editing (supporting)

Michelle Stern 0000-0003-3030-7065
Conceptualization (equal), Data curation (supporting), Formal analysis (supporting), Funding acquisition (lead), Investigation (supporting), Methodology (equal), Project administration (supporting), Supervision (equal), Visualization (supporting), Writing – original draft (supporting), Writing – review & editing (lead)

Lorraine E Flint
Conceptualization (supporting), Formal analysis (supporting), Methodology (supporting), Writing – review & editing (supporting)

Whitney Seymour 0000-0002-5999-6573
Data curation (equal), Formal analysis (supporting), Methodology (supporting), Project administration (supporting), Writing – review & editing (supporting)

References

Abatzoglou J T and Williams A P 2016 Impact of anthropogenic climate change on wildfire across western US forests *Proc. Natl Acad. Sci. USA* **113** 11770–5

Anderson E A 2006 *Snow accumulation and ablation model-SNOW-17* (U.S. National Weather Services) (available at: www.weather.gov/media/owp/oh/hrl/docs/22snow17.pdf) (Accessed 30 June 2024)

Bart R R, Tague C L and Moritz M A 2016 Effect of tree-to-shrub type conversion in lower montane forests of the Sierra Nevada (USA) on streamflow *PLoS One* **11** e0161805

Batjes N H, Calisto L and de Sousa L M 2024 WoSIS-latest: standardised world soil profile data. ISRIC soil data hub resource identifier *Date downloaded: 07/15/2022* (available at: https://tinyurl.com/39xhaa9d)

Blount K, Ruybal C J, Franz K J and Hogue T S 2020 Increased water yield and altered water partitioning follow wildfire in a forested catchment in the western United States *Ecohydrology* **13** 1–15

Boisramé G F S, Thompson S E, Tague C and Stephens S L 2019 Restoring a natural fire regime alters the water balance of a sierra Nevada catchment *Water Resour. Res.* **55** 5751–69
Boisramé G, Thompson S, Collins B and Stephens S 2017 Managed wildfire effects on forest resilience and water in the Sierra Nevada *Ecosystems* **20** 717–32
Brown T C, Hobbins M T and Ramirez J A 2008 Spatial distribution of water supply in the coterminous United States *J. Am. Water Resour. Assoc.* **44** 1474–87
California Data Exchange Center 2024 Historical data selector (available at: https://cdec.water.ca.gov/dynamicapp/selectQuery) (Accessed June 30 2024)
California department of forest and fire protection CALFIRE 2015 *Fire and Resource Assessment Program (FRAP)* (available at: http://frap.fire.ca.gov/data/frapgisdata-subset)
California Department of Water Resources and US Bureau of Reclamation 2023 *Risk-informed future climate scenario development for the State Water Project delivery capability report*. (available at: https://data.cnra.ca.gov/dataset/d32744ae-2e11-4d6c-aa49-cc17085e4d30/resource/dffe00a6-017c-4765-affe-36b045c24969/download/risk-informed-future-climate-scenario-development-for-swp-dcr_final122023.pdf)
California Department of Water Resources 2018 *Hydroclimate report water year 2017*
California Department of Water Resources 2021 *Hydroclimate report water year 2020*
California Department of Water Resources 2022 *Hydroclimate report water year 2021*
California Department of Water Resources 2025a State water project (available at: https://water.ca.gov/programs/state-water-project)
California Department of Water Resources 2025b Snow surveys (available at: https://water.ca.gov/Programs/Flood-Management/Flood-Data/Snow-Surveys)
Caltabellotta G, Iovino M and Bagarello V 2022 Intensity and persistence of water repellency at different soil moisture contents and depths after a forest wildfire *J. Hydrol. Hydromech.* **70** 410–20
Carreras-Sospedra M, Zhu S, MacKinnon M, Lassman W, Mirocha J D, Barbato M and Dabdub D 2024 Air quality and health impacts of the 2020 wildfires in California *Fire Ecol.* **20** 1–22
Dahm C N, Colombano D D and Dahlgren R A 2025 Recent findings and future prospects for water quality effects from catastrophic wildfires in California, USA *San Franc. Estuary Watershed Sci.* **23** 1–28
Daly C, Halbleib M, Smith J I, Gibson W P, Doggett M K, Taylor G H, Curtis J and Pasteris P P 2008 Physiographically sensitive mapping of climatological temperature and precipitation across the conterminous United States *Int. J. Climatol.* **28** 2031–64
Debano L F 2000 The role of fire and soil heating on water repellency in wildland environments: a review *J. Hydrol.* **231** 195–206
DeBano L F, Neary D G and Ffolliott P F 1998 *Fire Effects on Ecosystems* (Wiley)
Doerr S H, Shakesby R A and MacDonald L H 2009 Soil water repellency: a key factor in post-fire erosion *Fire Effects on Soils and Restoration Strategies* (CRC Press) pp 213–40
Dow H W, East A E, Sankey J B, Warrick J A, Kostelnik J, Lindsay D N and Kean J W 2024 Postfire sediment mobilization and its downstream implications across California, 1984–2021 *J. Geophys. Res. Earth Surf.* **129** 1–23
Ebel B A 2020 Temporal evolution of measured and simulated infiltration following wildfire in the Colorado front range, USA: shifting thresholds of runoff generation and hydrologic hazards *J. Hydrol.* **585** 124765
Ebel B A and Moody J A 2017 Synthesis of soil-hydraulic properties and infiltration timescales in wildfire-affected soils *Hydrol. Process.* **31** 324–40
Ebel B A, Moody J A and Martin D A 2012 Hydrologic conditions controlling runoff generation immediately after wildfire *Water Resour. Res.* **48** W03529
Ebel B A, Shephard Z M, Walvoord M A, Murphy S F, Partridge T F and Perkins K S 2023 Modeling post-wildfire hydrologic response: review and future directions for applications of physically based distributed simulation *Earth's Future* **11** e2022EF003038
Eidenshink J, Schwind B, Brewer K, Zhu Z L, Quayle B and Howard S 2007 A project for monitoring trends in burn severity *Fire Ecol.* **3** 3–21
Escriva-Bou A, Medellin-azuara J, Hanak E, Abatzoglou J and Viers J 2022 Drought and California's Agriculture (*Public Policy Institute of California*)
Flint A L and Childs S W 1991 Use of the Priestley-Taylor evaporation equation for soil water limited conditions in a small forest clearcut *Agricultural and Forest Meteorology* **56** 247–60
Flint A L, Flint L E, Stern M A, Ackerly D A, Boynton R and Thorne J H 2024 Characterizing soil and bedrock water use of native California vegetation *Hydrology* **11** 22
Flint L E and Flint A L 2012 Downscaling future climate scenarios to fine scales for hydrologic and ecological modeling and analysis *Ecol. Process.* **1** 2
Flint L E, Flint A L and Stern M A 2021 The basin characterization model—A regional water balance software package (No. 6-H1) (U.S. Geological Survey) (https://doi.org/10.3133/tm6H1)
Furniss T, Hessburg P, Churchill D J, Wigmosta M S, Povak N, Duan Z and Salter R B 2025 Wildfire and forest treatments mitigate–but cannot forestall–climate-driven changes in streamflow regimes in a western US mountain landscape *Environ. Res. Lett.* **20** 084039
George H, Lile D, Childers C, Noble C, Oilar A, Haworth K, Schmidt K and Miller G 2007 Upper feather river watershed (UFRW) irrigation discharge management program irrigated agricultural practices in UFRW
Goeking S A and Tarboton D G 2020 Forests and water yield: a synthesis of disturbance effects on streamflow and snowpack in Western coniferous forests *J. For.* **118** 172–92
Goss M, Swain D L, Abatzoglou J T, Sarhadi A, Kolden C A, Williams A P and Diffenbaugh N S 2020 Climate change is increasing the likelihood of extreme autumn wildfire conditions across California *Environ. Res. Lett.* **15** 094016
Hallema D W, Sun G, Caldwell P V, Norman S P, Cohen E C, Liu Y and McNulty S G 2018 Burned forests impact water supplies *Nat. Commun.* **9** 1307
Horton J D, San Juan C A and Stoeser D B 2017 The state geologic map compilation (SGMC) geodatabase of the conterminous United States (No. 1052) (U.S. Geological Survey) (https://doi.org/10.5066/P1A3DQZK)
Huang G and Kadir T 2016 Estimates of natural and unimpaired flows for the central valley of California: water years 1922–2014 (*California Department of Water Resources*)
Kampf S K, McGrath D, Sears M G, Fassnacht S R, Kiewiet L and Hammond J C 2022 Increasing wildfire impacts on snowpack in the western U.S *Proc. Natl Acad. Sci. USA* **119** e2200333119
Kinoshita A M and Hogue T S 2011 Spatial and temporal controls on post-fire hydrologic recovery in Southern California watersheds *Catena* **87** 240–52

Kinoshita A M and Hogue T S 2015 Increased dry season water yield in burned watersheds in Southern California *Environ. Res. Lett.* **10** 014003
Koczot K M, Jeton A E, McGurk B J and Dettinger M D 2005 Precipitation-runoff processes in the Feather River basin, northeastern California, and streamflow predictability, water years 1971-97 U.S. Geological Survey Scientific Investigations Report 2004–5202 p 92
Koshkin A L, Hatchett B J and Nolin A W 2022 Wildfire impacts on western United States snowpacks *Front. Water* **4** 971271
Lapides D A, Hahm W J, Rempe D M, Whiting J and Dralle D N 2022 Causes of missing snowmelt following drought *Geophys. Res. Lett.* **49** e2022GL100505
Larsen I J, MacDonald L H, Brown E, Rough D, Welsh M J, Pietraszek J H, Libohova Z, de Dios Benavides-solorio J and Schaffrath K 2009 Causes of post-fire runoff and erosion: water repellency, cover, or soil sealing? *Soil Sci. Soc. Am. J.* **73** 1393–407
Loverin J K, Xi W, Su H and Zhang J 2024 Thinning and managed burning enhance forest resilience in northeastern California *Ecosyst. Health Sustain.* **10** 0164
Luković J, Chiang J C H, Blagojević D and Sekulić A 2021 A later onset of the rainy season in California *Geophys. Res. Lett.* **48** e2020GL090350
Ma Q, Bales R C, Rungee J, Conklin M H, Collins B M and Goulden M L 2020 Wildfire controls on evapotranspiration in California's Sierra Nevada *J. Hydrol.* **590** 125364
MacDonald G *et al* 2023 Drivers of California's changing wildfires: a state-of-the-knowledge synthesis *Int. J. Wildland Fire* **32** 1039–58
Magliozzi L J *et al* 2024 Wildland-urban interface wildfire increases metal contributions to stormwater runoff in Paradise, California *Environ. Sci.: Process. Impacts* **26** 667–85
Massmann A, Gentine P and Lin C 2019 When does vapor pressure deficit drive or reduce evapotranspiration? *J. Adv. Model. Earth Syst.* **11** 3305–20
Mayor A G, Bautista S, Llovet J and Bellot J 2007 Post-fire hydrological and erosional responses of a Mediterranean landscape: seven years of catchment-scale dynamics *Catena* **71** 68–75
Michaelis A C, Gershunov A, Weyant A, Fish M A, Shulgina T and Ralph F M 2022 Atmospheric river precipitation enhanced by climate change: a case study of the storm that contributed to california's oroville dam crisis *Earth's Future* **10** e2021EF002537
Moazeni S and Cerdà A 2024 The impacts of forest fires on watershed hydrological response. A review *Trees, Forests and People* **18** 100707
Moody J A, Ebel B A, Nyman P, Martin D A, Stoof C and McKinley R 2016 Relations between soil hydraulic properties and burn severity *Int. J. Wildland Fire* **25** 279–93
Mu Q, Zhao M and Running S W 2011 Improvements to a MODIS global terrestrial evapotranspiration algorithm *Remote Sens. Environ.* **115** 1781–800
Nelson K 2022 Burn severity portal, a clearing house of fire severity and extent information (ver. 12, December 2025) *US Geological Survey (USGS)* (https://doi.org/10.5066/P97UMU6K)
Niemeyer R J, Bladon K D and Woodsmith R D 2020 Long-term hydrologic recovery after wildfire and post-fire forest management in the interior Pacific Northwest *Hydrol. Process.* **34** 1182–97
Partington D *et al* 2022 Predicting wildfire induced changes to runoff: a review and synthesis of modeling approaches *Wiley Interdiscip. Rev.: Water* **9** e1599
Peterson C, Escriva-Bou A, Medellín-azuara J and Cole S 2023 *Water Use in California's Agriculture* (*Public Policy Institute of California*)
Priestley C H B and Taylor R J 1972 On the assessment of surface heat flux and evaporation using large-scale parameters *Mon. Weather Rev.* **100** 81–92
Reitz M, Sanford W E, Senay G B and Cazenas J 2017 Annual estimates of recharge, quick-flow runoff, and evapotranspiration for the contiguous U.S. using empirical regression equations *J. Am. Water Resour. Assoc.* **53** 961–83
Robles M D, Marshall R M, O'donnell F, Smith E B, Haney J A and Gori D F 2014 Effects of climate variability and accelerated forest thinning on watershed-scale runoff in southwestern USA ponderosa pine forests *PLoS One* **9** e111092
Roche J W, Ma Q, Rungee J and Bales R C 2020 Evapotranspiration mapping for forest management in California's Sierra Nevada *Front. For. Glob. Change* vol 3 p 69
Running S, Mu Q, Zhao M and Moreno A 2021 *MODIS/terra net evapotranspiration gap-filled yearly L4 global 500m SIN grid V061* [Dataset] (https://doi.org/10.5067/MODIS/MOD16A3GF.061)
Rust A J, Hogue T S, Saxe S and McCray J 2018 Post-fire water-quality response in the western United States *Int. J. Wildland Fire* **27** 203–16
Safford H D, Butz R J, Bohlman G N, Coppoletta M, Estes B L, Gross S E, Merriam K E and Wuenschel A 2021 Fire ecology of the North American Mediterranean-climate zone. chapter 7 *Fire Ecology and Management: Past, Present, and Future of US Forested Ecosystems* ed B Collins and C H Greenberg (Springer)
Safford H D, Paulson A K, Steel Z L, Young D J N and Wayman R B 2022 The 2020 California fire season: a year like no other, a return to the past or a harbinger of the future? *Glob. Ecol. Biogeogr.* **31** 2005–25
Santi P M and Morandi L 2013 Comparison of debris-flow volumes from burned and unburned areas *Landslides* **10** 757–69
Saxe S, Hogue T S and Hay L 2018 Characterization and evaluation of controls on post-fire streamflow response across western US watersheds *Hydrol. Earth Syst. Sci. Sciences* **22** 1221–37
Shen H, Tolson B A and Mai J 2022 Time to update the split-sample approach in hydrological model calibration *Water Resour. Res.* **58** e2021WR031523
Smith H G, Sheridan G J, Lane P N J, Nyman P and Haydon S 2011 Wildfire effects on water quality in forest catchments: a review with implications for water supply *J. Hydrol.* **396** 170–92
Stern M A, Seymour W A and Zamora-Reyes D 2026 Upper feather river watershed 30-meter basin characterization model—monthly historical climate and hydrology: U.S. geological survey data release (https://doi.org/10.5066/P138MUCW)
Stern M, Flint L, Minear J, Flint A and Wright S 2016 Characterizing changes in streamflow and sediment supply in the sacramento River Basin, California, using hydrological simulation program—FORTRAN (HSPF) *Water* **8** 432
Sun G, Caldwell P V and McNulty S G 2015 Modelling the potential role of forest thinning in maintaining water supplies under a changing climate across the conterminous United States *Hydrol. Process.* **29** 5016–30
Swain D L 2021 A shorter, sharper rainy season amplifies California OBUWildfire risk *Geophys. Res. Lett.* **48** e2021GL092843
Swain D L, Langenbrunner B, Neelin J D and Hall A 2018 Increasing precipitation volatility in twenty-first-century California *Nat. Clim. Change* **8** 427–33
Tague C L, Moritz M and Hanan E 2019 The changing water cycle: the eco-hydrologic impacts of forest density reduction in Mediterranean (seasonally dry) regions *Wiley Interdiscip. Rev.: Water* **6** e1350

Taylor A H and Beaty R M 2005 Climatic influences on fire regimes in the Northern Sierra Nevada mountains, Lake Tahoe Basin, Nevada, USA *J. Biogeogr.* **32** 425–38
Taylor A H, Harris L B and Skinner C N 2022 Severity patterns of the 2021 Dixie Fire exemplify the need to increase low-severity fire treatments in California's forests *Environ. Res. Lett.* **17** 071002
Tinebra I, Alagna V, Iovino M and Bagarello V 2019 Comparing different application procedures of the water drop penetration time test to assess soil water repellency in a fire affected Sicilian area *Catena* **177** 41–8
Touma D, Stevenson S, Swain D L, Singh D, Kalashnikov D A and Huang X 2022 Climate change increases risk of extreme rainfall following wildfire in the western United States *Sci. Adv.* **8** eabm0320
Ukasha M, Ramirez J A and Niemann J D 2022 Temporal variations of NDVI and LAI and interactions with hydroclimatic variables in a large and agro-ecologically diverse region *J. Geophys. Res.-Biogeosci.* **127** e2021JG006395
US Geological Survey 2022 3D elevation program 30-meter resolution digital elevation model (published 20200606) (available at: www.usgs.gov/the-national-map-data-delivery) (Accessed 30th June 2023)
US Geological Survey 2024 USGS water data for the nation: U.S *Geological Survey National Water Information System Database* (https://doi.org/10.5066/F7P55KJN) (Accessed July 2024)
Vieira D C S, Fernández C, Vega J A and Keizer J J 2015 Does soil burn severity affect the post-fire runoff and interrill erosion response? A review based on meta-analysis of field rainfall simulation data *J. Hydrol.* **523** 452–64
Walters A, Fang B and Lakshmi V 2024 Using earth observations to measure hydrological conditions before, during, and after wildfires in the feather river watershed *IEEE J. Sel. Top. Appl. Earth Obs. Remote Sens.* **17** 6972–85
Wells R, Mankin K R, Niemann J D, Kipka H, Green T R and Barnard D M 2024 Estimating changes in streamflow attributable to wildfire in multiple watersheds using a semi-distributed watershed model *Ecohydrology* **17**
Williams A P *et al* 2022 Growing impact of wildfire on western US water supply *Proc. Natl Acad. Sci. USA* **119** 1
Wine M L, Makhnin O and Cadol D 2018 Nonlinear long-term large watershed hydrologic response to wildfire and climatic dynamics locally increases water yields *Earth's Future* **6** 997–1006
Wu J, Baartman J E M and Nunes J P 2021 Comparing the impacts of wildfire and meteorological variability on hydrological and erosion responses in a Mediterranean catchment *Land Degrad. Dev.* **32** 640–53
Zamora-Reyes D, Black B and Trouet V 2022 Enhanced winter, spring, and summer hydroclimate variability across California from 1940 to 2019 *Int. J. Climatol.* **42** 4940–52